



# Atmospheric Chemistry – Chlorine Chemistry

Comparison of amine+Cl and  
amine+Br chemistry

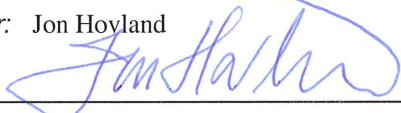
**Tel-Tek report no. 2211030-CC08 v2**

Claus Jørgen Nielsen,  
Arne Joakim Coldevin Bunkan, Yizhen Tang  
25.05.2012

Tel-Tek  
Kjølnes ring 30  
NO-3918 Porsgrunn  
NORWAY



## REFERENCE PAGE

<i>Author(s)</i> Claus Jørgen Nielsen, Arne Joakim Coldevin, Bunkan, Yizhen Tang	<i>Report no.</i> 2211030-CC08 v2	<i>Date</i> 25.05.2012
	<i>Classificaton*</i> Internal	
	<i>Pages/ Appendices</i> 40/1	
<i>Report Title</i> <b>Atmospheric Chemistry – Chlorine Chemistry</b>	<i>Subtitle</i> Comparison of amine+Cl and amine+Br chemistry	
	<i>Tel-Tek project no</i> 2211030	
<i>Report prepared for</i> Gassnova SF, contract no. 257430177, continued as Statoil Petroleum AS, contract no 4502450412	<i>Contact person</i> Steinar Pedersen	
<i>Abstract</i> The importance of atmospheric gas phase removal of amines by reaction with Br atoms in the Mongstad area has been evaluated employing <i>upper</i> limit rate coefficients to reaction from quantum chemistry calculations, and <i>upper</i> limit Br atom concentrations from SPACCIM model simulations of a mixed marine-urban scenario. The results show that Br atom reactions will only be important for the atmospheric loss of tertiary amines. It is concluded that there is no need for further studies of amine + Br reactions in connection with amine chemistry implementation in dispersion modelling of emissions from Mongstad.		
We have reviewed this report and find it in accordance with Tel-Tek's quality system		
<i>Project leader:</i> Jon Hoyland <i>Signature:</i> 	<i>Department leader:</i> Hans Aksel Haugen <i>Signature:</i> 	
<i>Keywords</i>		
<i>English</i> Amine Chlorine Bromine Kinetic	<i>Norwegian</i>	
*Classification: <b>Open</b> – report can be cited, given proper citation, <b>Internal</b> – report is internal, <b>Confidential</b>		

## About the Atmospheric Chemistry project

Gassnova has awarded Tel-Tek a contract (no. 257430177) for the project "Atmospheric chemistry". As of 1<sup>st</sup> April 2012 the project has been transferred to Statoil Petroleum AS (no. 4502450412). The project has four sub-projects:

- Aqueous phase chemistry
- Nitrosamine photolysis
- Dark chemistry
- Chlorine chemistry

Tel-Tek has entered a consortium agreement with universities and research institutions to carry out the project:

- University of Oslo. Norway
- Leibniz-Institut für Troposphärenforschung. Germany
- Universität Innsbruck. Austria
- IRCELYON. France
- Universidad de Castilla-La Mancha. Spain
- Georgia Tech. USA
- Norwegian University of Life Sciences. Norway

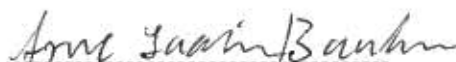
## Quality Assurance

The data and results in this report has been quality controlled and verified according to generally accepted principles for publication in internationally recognised scientific journals. This statement also includes the reports within the project that is used as a basis for the conclusions and recommendations in this report.

There is a vast amount of data available from the theoretical calculations, and most of this information is presented in a condensed graphical form. The original data are available upon request.



Claus J. Nielsen  
University of Oslo



Arne Joakim Coldevin Bunkan  
University of Oslo

Yizhen Tang  
University of Oslo

Dr. Tang is at the moment  
in China and could not sign

## CONTENTS

1	Objectives and scope of work .....	5
1.1	Scope of work .....	5
2	Quantum chemistry Calculations .....	6
2.1	Spin-Orbit Coupling.....	7
2.2	Enthalpies and Gibbs energies of reaction.....	7
2.3	Potential energy surfaces of amine + Cl reactions.....	10
2.4	Summary of QCC study of amine + Cl reactions .....	12
2.5	Potential energy surfaces of amine + Br reactions.....	13
2.6	Summary of QCC study of amine + Br reactions .....	15
2.7	Conclusions from QCC studies of amine + halogen.....	15
3	Kinetics of Br atom reactions with amines .....	16
4	OH, Cl and Br concentrations in the Mongstad area.....	19
5	Box model calculations of amine + OH, Cl and Br reactions.....	22
5.1	Model results for the period around Winter Solstice .....	23
5.2	Model results for the period around Spring Equinox.....	27
5.3	Model results for the period around Summer Solstice.....	31
6	Conclusions and recommendations.....	35
7	Literature .....	36
	Annex 1. Experimental Enthalpies of Formation.....	40

## 1 OBJECTIVES AND SCOPE OF WORK

The objective is to assess the importance of bromine atom reactions with amines in the Mongstad area.

The motivation for studying amine + bromine reactions is found in the Tel-Tek report no. 2211030-CC02, *Halogen Chemistry in the Mongstad Region: Literature Study and Model Simulations*.<sup>1</sup> In the summary of this report is stated:

Model simulations to specify halogen chemistry at Mongstad were conducted using the box model SPACCIM. Three scenarios were created representing air above an ocean (far from major pollutants) and mixtures of this clean marine air with remote continental and urban air, respectively. Halogen chemistry can only be described adequately, when aqueous phase processes are taken into account. Between gas-phase-only and full chemistry runs, Cl- and Br-concentrations differ by a factor of 10-100. Halogen atom concentrations are at the lower end (Cl) or below (Br) the range of measured values, which is due to a lack of emitted halogen species contained in sea-salt. The Br-concentration is expected to be about 1 or 2 orders of magnitude higher than simulated.

A relationship between reactive halogen species and halogen-nitrogen species was observed. Beneath X<sub>2</sub> halogen-nitrates and -nitrites are reservoir species, which are photolysed rapidly and release reactive halogens.

Because of the importance of NO<sub>x</sub> for halogen chemistry (via build up of halogen-nitrates and nitrites), the marine-urban scenario, where NO<sub>x</sub>-levels are in the range of measurements at Mongstad, should give the best estimate for Mongstad halogen conditions. In that run Cl reaches concentrations up to  $8 \times 10^3$  molecules/cm<sup>3</sup>. The Br peak-concentration is about  $2 \times 10^4$  molec/cm<sup>3</sup>, but is expected to be higher in reality (see above).

In winter photolysis occurs with less intensity and only for a short period during the day. Therefore reactive halogen species do not reach the levels of the summer cases. Increasing the intensity of photolysis on a summer day leads to slightly higher peak-concentrations of reactive halogens.

### 1.1 Scope of work

UiO will undertake a comparative quantum chemistry study of the Br and Cl atom reactions with simple amines, using already obtained kinetic data for the reaction of Cl with methyl-, dimethyl- and trimethylamine as fix points for the calculations.

The importance of Cl and Br atom reactions with amines in the Mongstad area will be illustrated by box-model calculations and compared the corresponding OH radical reactions. A recommendation on if and how Br atom reactions should be included in future dispersion model simulations will be given.

## 2 QUANTUM CHEMISTRY CALCULATIONS

Various types of Quantum Chemistry Calculations (QCC) in combination with different basis sets were used in an initial characterisation of the  $\text{CH}_3\text{NH}_2+\text{Cl}$  and  $\text{CH}_3\text{NH}_2+\text{Br}$  reactions to establish a common method for the study. All calculations were carried out with the Gaussian 03<sup>2</sup> and 09<sup>3</sup> program suites.

The following conclusions were drawn from the exploratory calculations:

- Density functional theory (DFT) methods are generally computational cost-effective and give approximate structures of stationary points on the potential energy surface of a reaction system. However, DFT methods were unable to locate all transition states for the amine+Cl and amine+Br reaction systems. In short, DFT methods could not be used in a general study of Cl and Br reactions with amines.
- MP2<sup>4-8</sup> (second order Møller-Plesset perturbation) calculations are considered one step up the QCC hierarchy. MP2 calculations are more costly in terms of CPU-time, but can in principle be carried out in a matter of days for the present systems. However, the MP2 method fails for some of the steps in the amine+Br reactions. Consequently, MP2 calculations could not be used in a general study of Cl and Br reactions with amines.
- The more robust, but also more CPU-expensive CCD,<sup>9</sup> CCSD,<sup>10-13</sup> and QCISD<sup>14</sup> methods perform well in locating the stationary points on the potential energy surfaces of the amine+Cl and amine+Br reactions. It was decided to use a medium-sized basis set of double zeta quality (aug-cc-pVDZ<sup>15-18</sup>) to locate and optimize structures of stationary points on the reaction hyper surfaces. After comparing results obtained for the  $\text{CH}_3\text{NH}_2+\text{Cl}$  system by the three methods, it was decided to use CCSD as the common method for all reaction systems.
- Higher level electron correlation methods, CCSD(T)<sup>14</sup> and QCISD(T),<sup>14</sup> were employed to improve the calculated energies in single point calculations using the aug-cc-pVTZ triple zeta quality basis set.<sup>15-18</sup> After comparing results obtained for the  $\text{CH}_3\text{NH}_2+\text{Cl}$  system by the two methods, it was decided to use CCSD(T) as the common method for all systems.

The stationary points on the potential energy hyper-surfaces were unambiguously identified as minima (number of imaginary vibrational frequencies = 0) or as transition states (number of imaginary vibrational frequencies = 1). The minimum energy paths from reactants to products on the potential energy hyper-surfaces were mapped employing the intrinsic reaction coordinate method (IRC) method of Gonzales and Schlegel.<sup>19</sup> The IRC calculations were carried out in mass-weighted Cartesian coordinates using a step size of  $0.02 \text{ u}^{1/2} \text{ bohr}$ .

## 2.1 Spin-Orbit Coupling

Spin-orbit (SO) coupling in the Cl and Br atoms results in a splitting of the atom ground configuration into  $^2P_{3/2}$  and  $^2P_{1/2}$  states separated by 882.36 and 3685.24  $\text{cm}^{-1}$ , respectively.<sup>20</sup> This splitting changes during reaction and should therefore be included in the potential energy function. Assuming that SO coupling is only relevant in the reactant region as found for the Cl + HCl reaction system,<sup>21</sup> the SO coupling will lower the asymptotic potential energy of the reactants by 1/3 of the SO splitting (294.12  $\text{cm}^{-1} = 3.52 \text{ kJ mol}^{-1}$  for the amine + Cl reactions and 1228.41  $\text{cm}^{-1} = 14.69 \text{ kJ mol}^{-1}$  for the amine + Br reactions). Figure 2.1 illustrates how the SO coupling in Cl changes as a function of reaction coordinate.

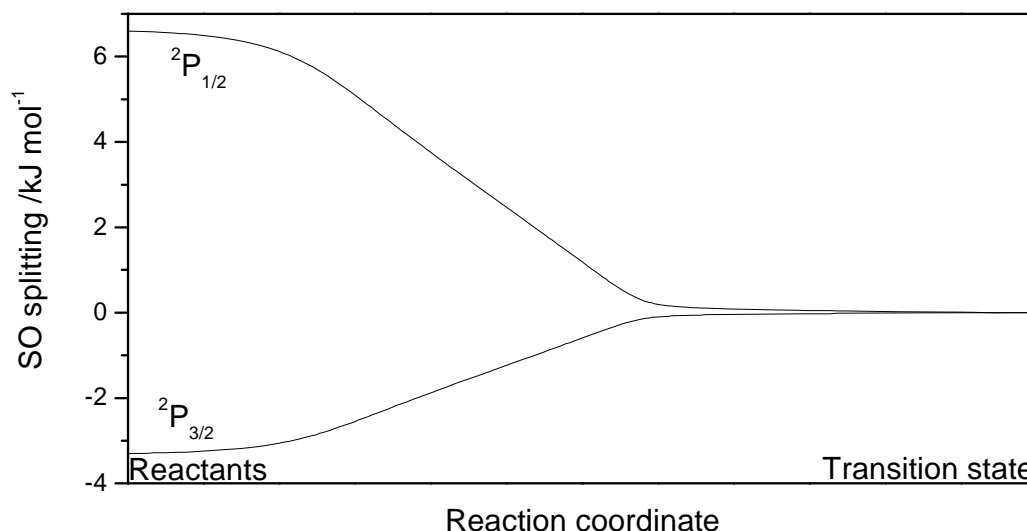


Figure 2.1. SO splitting in Cl as a function of reaction coordinate on the minimum energy path from reactants to transition state.

## 2.2 Enthalpies and Gibbs energies of reaction

The model chemistries CBS-QB3,<sup>22</sup> G3,<sup>23</sup> and G4<sup>24</sup> were used to obtain thermochemistry information. The CBS-QB3 method uses B3LYP<sup>25-28</sup> hybrid density functional geometries and frequencies, the G3 method uses HF frequencies and MP2 geometries. The G4 method is a composite method that includes higher-level corrections to account for deficiencies in the G3 energy calculations. The G4 method is assessed on the 454 experimental energies in the G3/05 test set,<sup>29</sup> and the average absolute deviation from experiment is only 3.5  $\text{kJ mol}^{-1}$  (G3 theory: 4.7  $\text{kJ mol}^{-1}$ ). Both the G3 and G4 methods include a spin-orbit term taken from experiment; the G4 method is currently considered one of the most accurate tools for calculation of thermochemistry.

The enthalpy of a chemical bond R—X is defined by the reaction:



Bond enthalpies are therefore a special case of the general reaction enthalpy. There are only few experimental bond enthalpies available for amines, and in most cases they have large uncertainties.<sup>#</sup> However, the available relevant bond enthalpies validate the theoretical methods employed; Table 2.1 compares C-H and N-H bond enthalpies in amines to results from QCC. In general, the agreement between experimental and theoretical bond enthalpies is

<sup>#</sup> Relevant experimental enthalpies of formation are found in ANNEX 1, page 49.

very good. There are, however, significant discrepancies (25 – 35 kJ mol<sup>-1</sup>) between experimental and theoretical values for the C-H bond enthalpies in dimethylamine and trimethylamine. There is only a single experimental study of enthalpy of formation of the CH<sub>3</sub>NHCH<sub>2</sub> and (CH<sub>3</sub>)<sub>2</sub>NCH<sub>2</sub> radicals, and all QCC studies carried out indicate that the experimental values for these species are subject to large, systematic errors.

Table 2.1. Experimental bond enthalpies and results from quantum chemistry calculations.

Amine	$\Delta_{\text{bond}}H / \text{kJ mol}^{-1}$				
	Experimental	CBS-QB3	G3	G4	CCSD(T) <sup>a</sup>
HCl	431.6 <sup>30</sup>	436	431	430	421
HBr	372.4 <sup>30</sup>	385	366	364	365
CH <sub>3</sub> NH <sub>2</sub>	416.7 <sup>31</sup> ; 418 ± 10 <sup>32</sup>	419	417	414	411
CH <sub>3</sub> NH <sub>2</sub>	390.6 <sup>31</sup> ; 390 ± 8 <sup>32</sup>	391	389	388	386
(CH <sub>3</sub> ) <sub>2</sub> NH	383 ± 8 <sup>32</sup>	395	394	390	385
(CH <sub>3</sub> ) <sub>2</sub> NH	364 ± 8 <sup>32</sup>	389	387	385	384
(CH <sub>3</sub> ) <sub>3</sub> N	351 ± 8 <sup>32</sup>	389	388	384	385
CH <sub>3</sub> CH <sub>2</sub> NH <sub>2</sub>	414.2 <sup>31</sup>	428			
CH <sub>3</sub> CH <sub>2</sub> NH <sub>2</sub>	376.8 <sup>31</sup>	386			
CH <sub>3</sub> CH <sub>2</sub> NH <sub>2</sub>	413.0 <sup>31</sup>	419			
(CH <sub>3</sub> ) <sub>3</sub> CNH <sub>2</sub>	406.6 <sup>31</sup>	424			

<sup>a</sup> Results from CCSD(T)/aug-cc-pVTZ//CCSD/aug-cc-pVDZ calculations.

Experimental and theoretical reaction enthalpies at 298.15 K for the methyl- dimethyl- and trimethylamine reactions with Cl and Br atoms are compared in Table 2.2. It can be seen that all amine + Cl atoms reactions are exothermic at 298.15 K, while all amine + Br atom reactions are all endothermic. It is noted that the enthalpies of reaction obtained in CCSD(T)/aug-cc-pVTZ//CCSD/aug-cc-pVDZ calculations, which are used in the study of the amine + Cl/Br potential energy reaction surfaces (see later), appear systematically smaller than the more accurate G3 and G4 values. This is essentially caused by a too small basis set used in the CC-calculations; it is not feasible with the present technology to carry out CC-calculations on the amine+Br reactions with larger basis sets (a single point CCSD(T)/aug-cc-pVTZ calculation on a stationary point on the trimethylamine+Br reaction hyper surface requires around 1 month CPU-time).<sup>#</sup>

Table 2.3 summarizes the QCC results for Gibbs energies of the amine + Cl/Br reactions; the amine + Cl reactions are all exergonic while the amine + Br reactions are all endergonic.

The previously mentioned discrepancies between experimental and theoretical C-H bond enthalpies in dimethylamine and trimethylamine are also seen as discrepancies between experimental and theoretical reaction enthalpies involving the CH<sub>3</sub>NHCH<sub>2</sub> and (CH<sub>3</sub>)<sub>2</sub>NCH<sub>2</sub> radicals.

<sup>#</sup> DFT and MP2 methods fail in locating the transition states of the amine + Br reactions. The CBS-QB3, G3 and G4 model chemistries therefore cannot be used to calculate the energies of the transition states in the amine + Br reactions.

Table 2.2. Experimental enthalpies of reaction at 298.15 K and results from quantum chemistry calculations.

Reaction	Exp.	$\Delta H_{298}^{\theta} / \text{kJ} \cdot \text{mol}^{-1}$			
		CBS-QB3	G3	G4	CCSD(T) <sup>a</sup>
$\text{CH}_3\text{NH}_2 + \text{Cl} \rightarrow \text{CH}_2\text{NH}_2 + \text{HCl}$	-41.2	-45.4	-41.5	-41.9	-34.8
$\text{CH}_3\text{NH}_2 + \text{Cl} \rightarrow \text{CH}_3\text{NH} + \text{HCl}$	-13.2	-17.5	-14.1	-15.3	-9.9
$(\text{CH}_3)_2\text{NH} + \text{Cl} \rightarrow \text{CH}_3\text{NHCH}_2 + \text{HCl}$	-69.5	-47.6	-43.4	-44.9	-36.1
$(\text{CH}_3)_2\text{NH} + \text{Cl} \rightarrow (\text{CH}_3)_2\text{N} + \text{HCl}$	-49.8	-41.5	-36.7	-39.4	-35.1
$(\text{CH}_3)_3\text{NH} + \text{Cl} \rightarrow (\text{CH}_3)_2\text{NCH}_2 + \text{HCl}$	-80.3	-47.7	-42.9	-45.8	-45.8
$\text{CH}_3\text{NH}_2 + \text{Br} \rightarrow \text{CH}_2\text{NH}_2 + \text{HBr}$	24.1	- <sup>b</sup>	23.1	23.8	21.3
$\text{CH}_3\text{NH}_2 + \text{Br} \rightarrow \text{CH}_3\text{NH} + \text{HBr}$	52.1	- <sup>b</sup>	50.5	50.4	46.2
$(\text{CH}_3)_2\text{NH} + \text{Br} \rightarrow \text{CH}_3\text{NHCH}_2 + \text{HBr}$	-4.2	- <sup>b</sup>	21.2	20.8	19.7
$(\text{CH}_3)_2\text{NH} + \text{Br} \rightarrow (\text{CH}_3)_2\text{N} + \text{HBr}$	15.5	- <sup>b</sup>	28.0	26.3	20.7
$(\text{CH}_3)_3\text{NH} + \text{Br} \rightarrow (\text{CH}_3)_2\text{NCH}_2 + \text{HBr}$	-15.0	- <sup>b</sup>	21.8	20.0	20.4

<sup>a</sup> Results from CCSD(T)/aug-cc-pVTZ//CCSD/aug-cc-pVDZ calculations including spin-orbit corrections. <sup>b</sup> Br atoms not included in the CBS-QB3 model chemistry.

Table 2.3. Gibbs free energies of reaction at 298.15 K from quantum chemistry calculations.

Reaction	$\Delta G_{298}^{\theta} / \text{kJ} \cdot \text{mol}^{-1}$			
	CBS-QB3	G3	G4	CCSD(T) <sup>a</sup>
$\text{CH}_3\text{NH}_2 + \text{Cl} \rightarrow \text{CH}_2\text{NH}_2 + \text{HCl}$	-54.3	-50.4	-50.9	-43.8
$\text{CH}_3\text{NH}_2 + \text{Cl} \rightarrow \text{CH}_3\text{NH} + \text{HCl}$	-27.2	-23.7	-25.0	-19.5
$(\text{CH}_3)_2\text{NH} + \text{Cl} \rightarrow \text{CH}_3\text{NHCH}_2 + \text{HCl}$	-57.5	-53.1	-54.9	-45.6
$(\text{CH}_3)_2\text{NH} + \text{Cl} \rightarrow (\text{CH}_3)_2\text{N} + \text{HCl}$	-55.4	-49.1	-52.9	-41.6
$(\text{CH}_3)_3\text{NH} + \text{Cl} \rightarrow (\text{CH}_3)_2\text{NCH}_2 + \text{HCl}$	-61.1	-53.3	-59.2	-58.9
$\text{CH}_3\text{NH}_2 + \text{Br} \rightarrow \text{CH}_2\text{NH}_2 + \text{HBr}$	- <sup>b</sup>	13.7	14.4	11.9
$\text{CH}_3\text{NH}_2 + \text{Br} \rightarrow \text{CH}_3\text{NH} + \text{HBr}$	- <sup>b</sup>	40.4	40.3	36.2
$(\text{CH}_3)_2\text{NH} + \text{Br} \rightarrow \text{CH}_3\text{NHCH}_2 + \text{HBr}$	- <sup>b</sup>	11.0	10.4	9.7
$(\text{CH}_3)_2\text{NH} + \text{Br} \rightarrow (\text{CH}_3)_2\text{N} + \text{HBr}$	- <sup>b</sup>	15.0	12.3	13.8
$(\text{CH}_3)_3\text{NH} + \text{Br} \rightarrow (\text{CH}_3)_2\text{NCH}_2 + \text{HBr}$	- <sup>b</sup>	10.8	6.1	6.8

<sup>a</sup> Results from CCSD(T)/aug-cc-pVTZ//CCSD/aug-cc-pVDZ calculations including spin-orbit corrections. <sup>b</sup> Br atoms not included in the CBS-QB3 model chemistry.

## 2.3 Potential energy surfaces of amine + Cl reactions

Rudic *et al.*<sup>33</sup> presented theoretical calculations (G2-level chemistry model<sup>34</sup>) on the methyl-amine + Cl reaction revealing transition states lower in energy than the reactants. Figure 2.2 shows a schematic diagram of the stationary points on the potential energy hyper-surface of the  $\text{CH}_3\text{NH}_2 + \text{Cl}$  reaction; the relative energies from CCSD(T)/aug-cc-pVTZ//CCSD/aug-cc-pVDZ calculations have been corrected for spin-orbit coupling in the Cl atom. The transition states to hydrogen abstractions from both the methyl- and amino-groups have lower energies than the reactants. The transition states to hydrogen abstraction from the methyl group and the amino group connect to the same pre-reaction adduct (PreRA) on the minimum energy paths (MEPs). On the product side, HCl forms post-reaction adducts (PostRA) before separation into products.

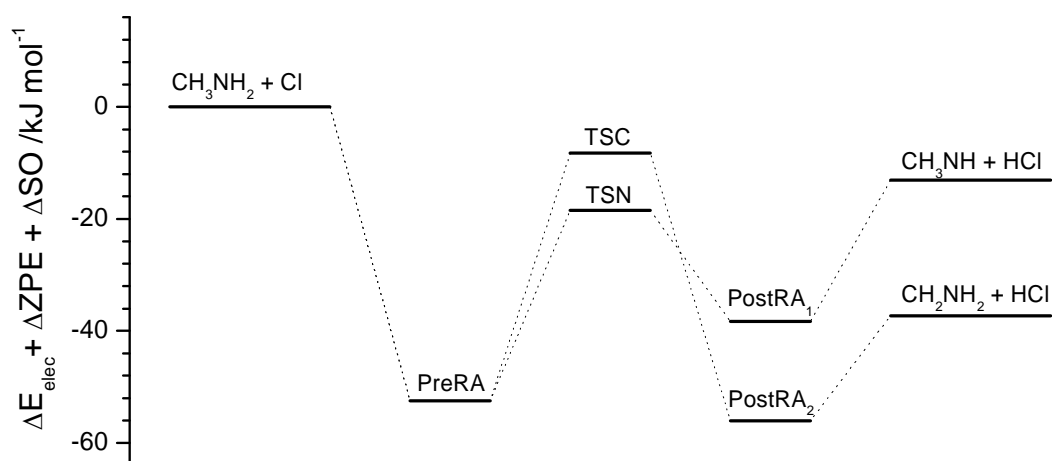


Figure 2.2. Energies of stationary points on the potential energy hyper surface and minimum energy paths of the  $\text{CH}_3\text{NH}_2 + \text{Cl}$  reaction. Results from CCSD(T)/aug-cc-pVTZ//CCSD/aug-cc-pVDZ calculations.

Figure 2.3 shows a schematic diagram of the stationary points on the potential energy hyper-surface of the  $(\text{CH}_3)_2\text{NH} + \text{Cl}$  reaction. The transition states to hydrogen abstractions from the methyl- and amino-groups have lower energies than the reactants and the MEPs to hydrogen abstraction occur via the same pre-reaction adduct (PreRA).

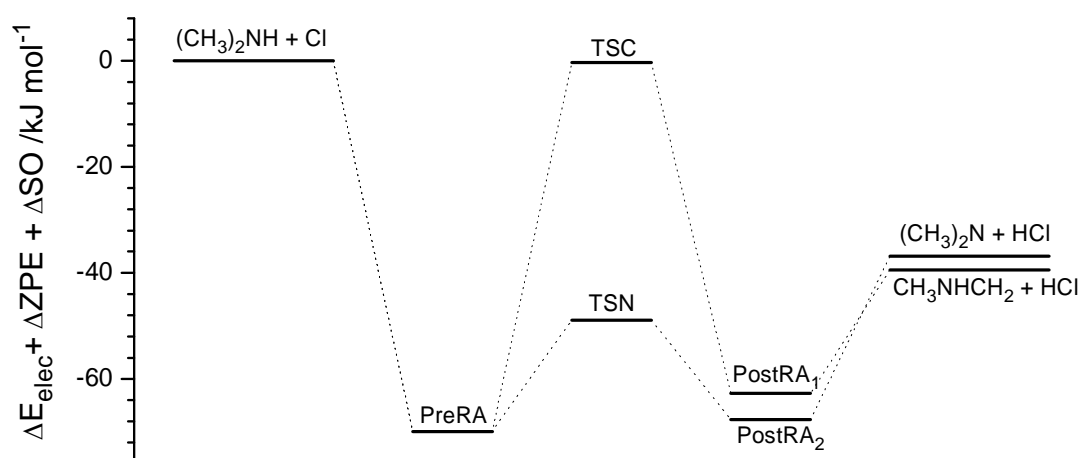


Figure 2.3. Energies of stationary points on the potential energy hyper surface and minimum energy paths of the  $(\text{CH}_3)_2\text{NH} + \text{Cl}$  reaction. Results from CCSD(T)/aug-cc-pVTZ//CCSD/aug-cc-pVDZ calculations.

It is noteworthy that the transition state to H-abstraction from the amino group in dimethylamine is much lower in energy than the TS to H-abstraction from the methyl group. On the product side, HCl forms post-reaction adducts (PostRA<sub>1</sub> and PostRA<sub>2</sub>) before separation into reactants.

A schematic diagram of the stationary points on the potential energy hyper-surface of the (CH<sub>3</sub>)<sub>2</sub>NH+Cl reaction is shown in Figure 2.4. The transition state to hydrogen abstractions from the methyl-group has a barely lower energy than the reactants. Again, the minimum energy path to hydrogen abstraction occur via a pre-reaction adduct (PreRA). On the product side, HCl forms a weakly bound post-reaction adduct (PostRA) before separation into reactants.

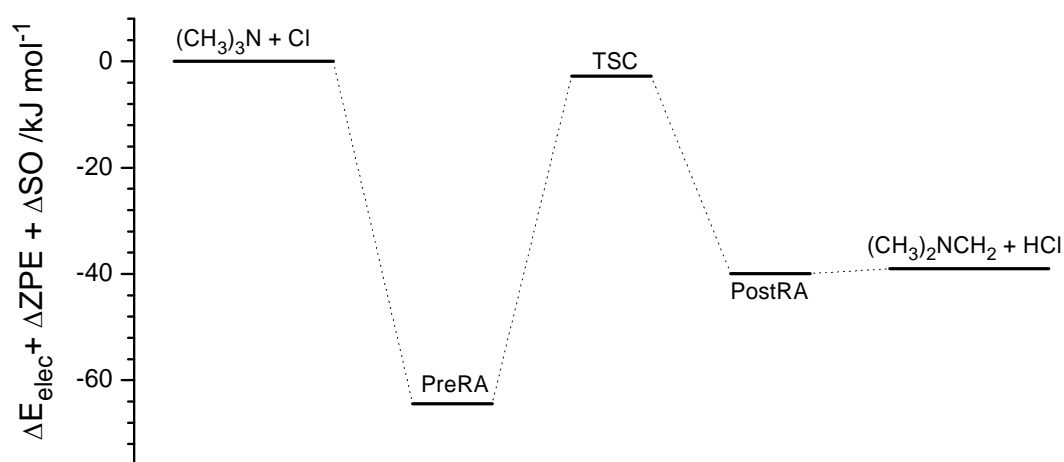


Figure 2.4. Energies of stationary points on the potential energy hyper surface and minimum energy paths of the (CH<sub>3</sub>)<sub>3</sub>N+Cl reaction. Results from CCSD(T)/aug-cc-pVTZ//CCSD/aug-cc-pVDZ calculations.

## 2.4 Summary of QCC study of amine + Cl reactions

The potential energy hypersurfaces of the three amine + Cl reactions all have pre-reaction adducts with energies around  $60 \text{ kJ mol}^{-1}$  below that of the reactants on the MEPs to the transition states. For comparison, the typical “strong” hydrogen bond between water and trimethylamine is only around  $25 \text{ kJ mol}^{-1}$ .<sup>35</sup> The structures of the pre-reaction adducts, shown in Figure 2.6, all have N-Cl distances of around  $2.37 \text{ \AA}$ .

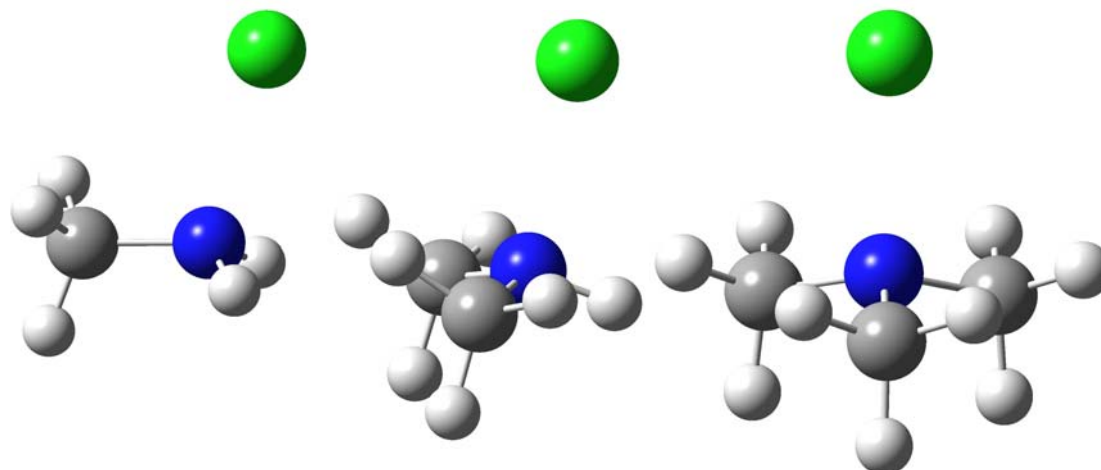


Figure 2.5. Structures of the pre-reaction complexes in the methyl-, dimethyl- and trimethylamine reactions with Cl atoms.

Rudic *et al.*<sup>33</sup> studied the dynamics of the Cl atom reaction with  $\text{CH}_3\text{NH}_2$ ,  $\text{CD}_3\text{NH}_2$ ,  $\text{CH}_3\text{ND}_2$  and  $\text{CD}_3\text{ND}_2$  and reported branching ratios for C-H:N-H and C-D:N-D abstraction to be 0.48:0.52 and 0.58:0.42, respectively. There are no data available for the branching in the initial step of Cl atom reaction with secondary amines. The present theoretical study suggests that hydrogen abstraction from the amino group should be the dominant route, and that Cl atom reaction with dimethylamine therefore could lead to more nitrosamine and nitramine formation than the corresponding OH reaction.

## 2.5 Potential energy surfaces of amine + Br reactions

Figure 2.6 shows a schematic diagram of the stationary points on the potential energy hyper-surface of the  $\text{CH}_3\text{NH}_2 + \text{Br}$  reaction; the relative energies from CCSD(T)/aug-cc-pVTZ//CCSD/aug-cc-pVDZ calculations have been corrected for spin-orbit coupling in the Br atom. The transition state to hydrogen abstraction from the methyl group is around  $9 \text{ kJ mol}^{-1}$  lower in energy than the reactants, whereas the TS to H-abstraction from the amino group is around  $18 \text{ kJ mol}^{-1}$  higher in energy than the reactants. Both transition states connect to the same pre-reaction adduct (PreRA) on the minimum energy paths (MEPs). On the product side, HBr forms weakly bound post-reaction adducts (PostRA) before separation into products. It should be noted that the potential surface is rather flat in the regions around the transition states.

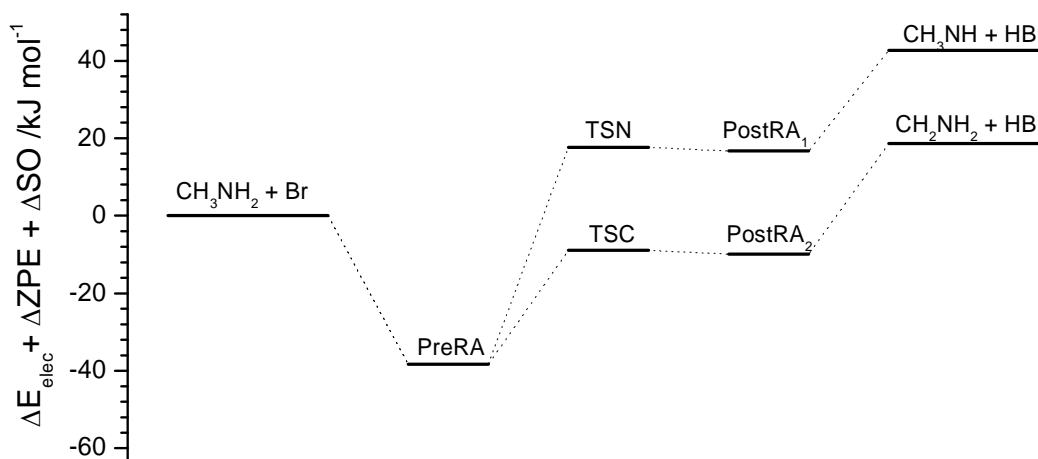


Figure 2.6. Energies of stationary points on the potential energy hyper surface and minimum energy paths of the  $\text{CH}_3\text{NH}_2 + \text{Br}$  reaction. Results from CCSD(T)/aug-cc-pVTZ//CCSD/aug-cc-pVDZ calculations.

Figure 2.7 shows a schematic diagram of the stationary points on the potential energy hyper-surface of the  $(\text{CH}_3)_2\text{NH} + \text{Br}$  reaction. The transition states to hydrogen abstractions from the methyl- and amino-groups both have lower energies than the reactants and the MEPs to hydrogen abstraction occur via the same pre-reaction adduct (PreRA). Again, it should be noted that the potential surface is rather flat in the region around the TSC transition state.

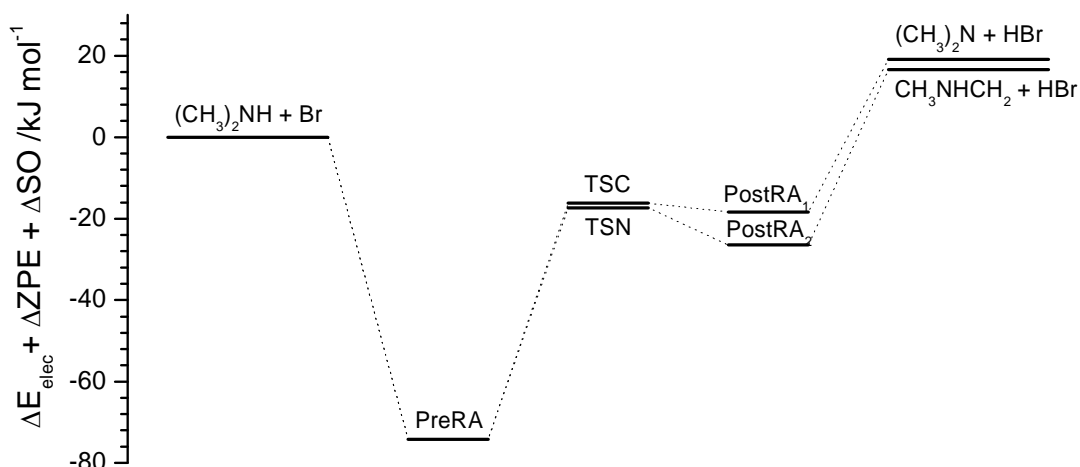


Figure 2.7. Energies of stationary points on the potential energy hyper surface and minimum energy paths of the  $(\text{CH}_3)_2\text{NH} + \text{Br}$  reaction. Results from CCSD(T)/aug-cc-pVTZ//CCSD/aug-cc-pVDZ calculations.

Figure 2.8 shows a schematic diagram of the stationary points on the potential energy hyper-surface of the  $(\text{CH}_3)_3\text{N}+\text{Br}$  reaction. The transition state to hydrogen abstractions from the methyl groups could not be located on the flat potential energy surface in CCD and CCSD calculations. It is known that energy must be around that of the post reaction adduct, PostRA, but the TSC-structure could, as mentioned, not be accurately located. Although not proven by IRC calculations, the MEPs to hydrogen abstraction is believed to occur via a pre-reaction adduct (PreRA).

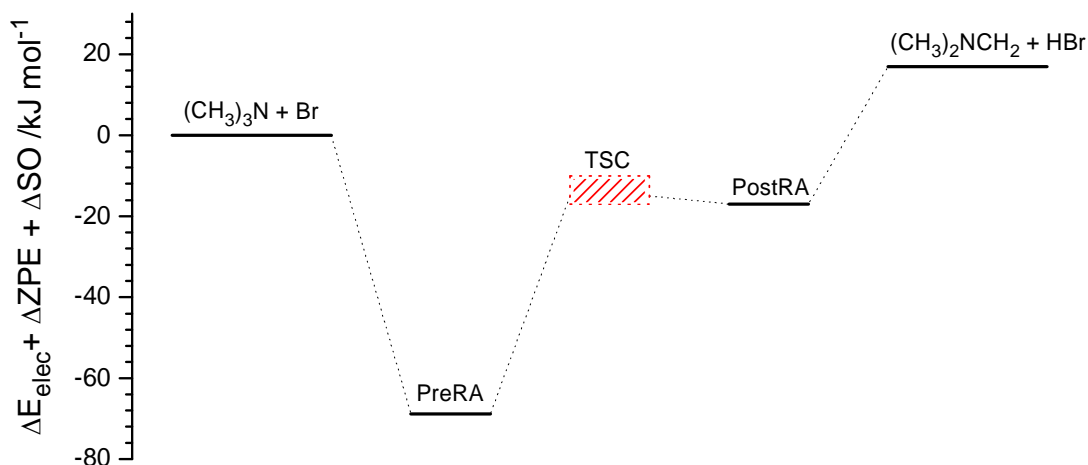


Figure 2.8.  $(\text{CH}_3)_3\text{N}+\text{Br}$ : structures of stationary points on the potential energy hyper surface. The transition state to H-abstraction could not be located. However, the energy of TSC must be in the range indicated.

Figure 2.9 shows a predicted energy diagram of the stationary points on the potential energy hyper-surface of the  $\text{NH}_2\text{CH}_2\text{CH}_2\text{OH}+\text{Br}$  as reaction resulting from G4 calculations. Approximate ranges to the energies of the pre-reaction adduct, the transition states and post reaction adducts are indicated. Note that hydrogen abstraction from the amino group in MEA by Br atoms is highly endothermic.

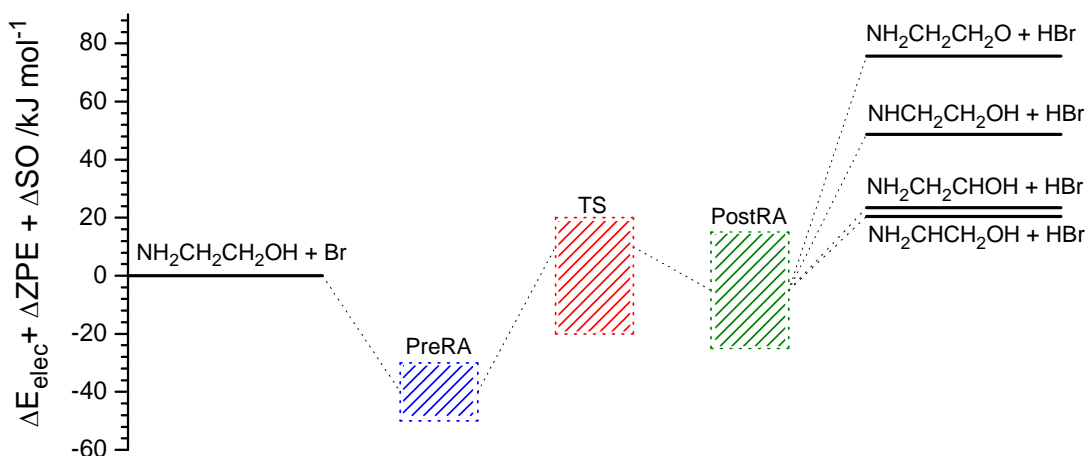


Figure 2.9. Energies of stationary points on the potential energy hyper surface and minimum energy paths of the  $\text{NH}_2\text{CH}_2\text{CH}_2\text{OH}+\text{Br}$  reaction. Results from G4 calculations.

## 2.6 Summary of QCC study of amine + Br reactions

The potential energy hypersurfaces of the methyl-, dimethyl- and trimethylamine + Br reactions all have strongly bonded pre-reaction adducts with energies 40 - 60 kJ mol<sup>-1</sup> below that of the reactants on the MEPs to the transition states. The structures of the pre-reaction adducts, shown in Figure 2.10, have N-Br distances of around 2.50 Å (2.53 Å in CH<sub>3</sub>NH<sub>2</sub>\*Br).

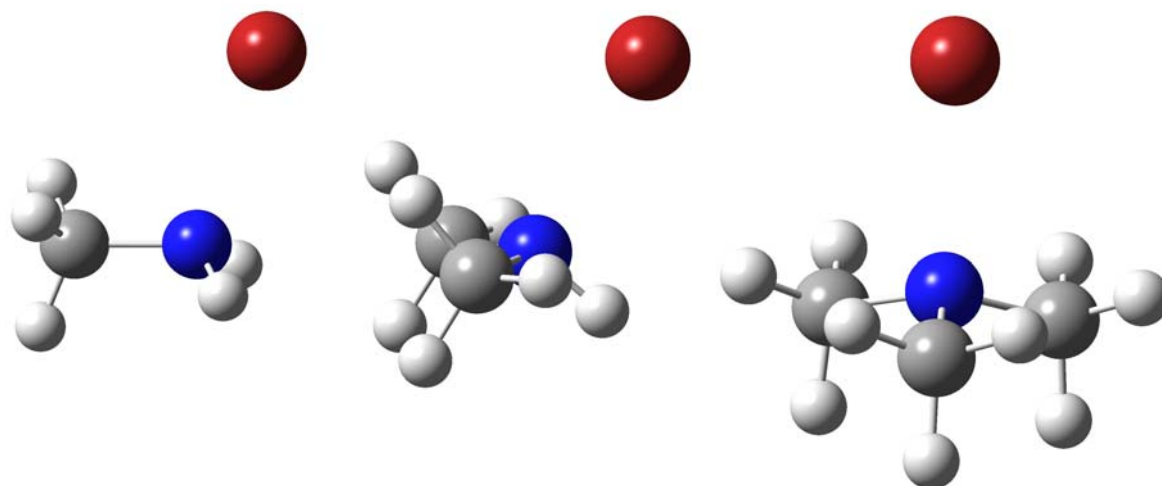


Figure 2.10. Structures of the pre-reaction complexes in the methyl-, dimethyl- and trimethylamine reactions with Br atoms.

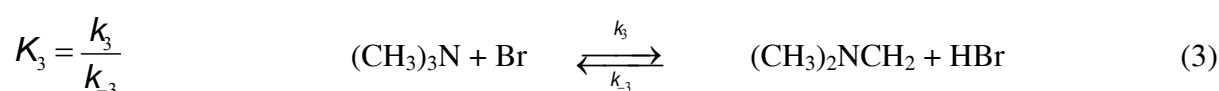
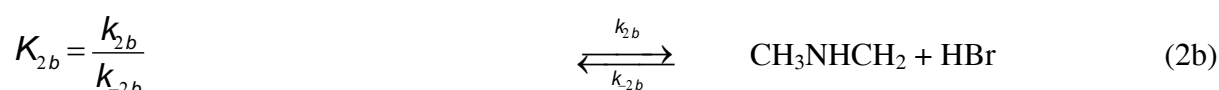
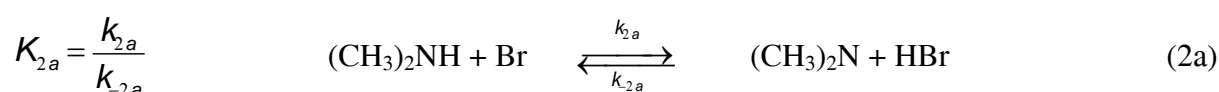
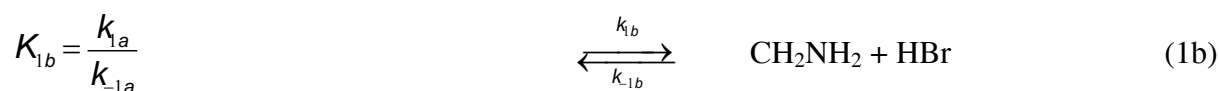
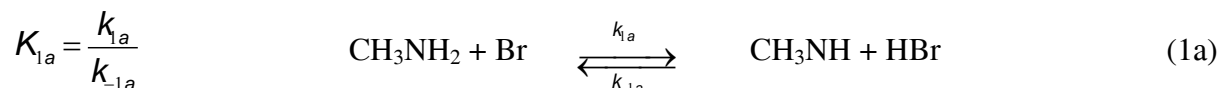
## 2.7 Conclusions from QCC studies of amine + halogen

The present QCC study shows that the potential energy hypersurfaces of amine reactions with Cl and Br atoms have one feature in common: they all involve a pre-reaction complex in which the halogen is strongly bonded to the lone-pair of the amino group. From then on the potential energy reaction hyper-surfaces of Cl and Br reactions with amines differ.

It has already been mentioned that all routes in the amine+Cl reactions are exothermic and exogenic, while the amine+Br reactions all are endothermic and endergonic. Further, all routes in the methyl-, dimethyl- and trimethylamine + Cl reactions occur without potential energy barriers above the entrance energies. The transition states to hydrogen abstraction from the methyl groups are lower by a few kJ mol<sup>-1</sup> in the Br reactions than in the corresponding Cl reactions, while the transition states to hydrogen abstraction from the amino groups are almost 40 kJ mol<sup>-1</sup> higher in the Br reactions than in the corresponding Cl reactions. This makes it futile to use results from amine+Cl kinetics modelling as anchor points for and amine+Br kinetics modelling.

### 3 KINETICS OF BR ATOM REACTIONS WITH AMINES

The potential energy hyper surfaces of the methyl-, dimethyl- and trimethylamine reactions with Br atoms are such that it is not valid to use any form of Transition State Theory to calculate the reaction rate coefficients. The reactions are all endergonic and the rate coefficients can then be determined from the reverse reaction rate coefficient making use of the relation between the thermodynamic equilibrium constant and the forward and reverse reaction rate coefficients:



The reverse reactions ( $k_{-1a}$ ,  $k_{-2a}$  and  $k_{-3}$ ) are all without potential energy barriers (see Figure 2.7, 2.9 and 2.11). Attempts to obtain reliable rate coefficients for the reverse reactions by solving the Master Equation for a multi energy-well system failed. It was therefore decided to settle for *upper* limits to the rate coefficients for the reverse reactions. In turn, these will then give *upper* limits to the forward reaction rate coefficients.

Simple collision theory gives *upper* limits to the reverse reactions:

$$k(T) = Z \cdot \exp\left(\frac{-E_a}{RT}\right) \quad ; \quad Z = N_A \cdot \sigma_{AB} \cdot \sqrt{\frac{8k_B T}{\pi \mu_{AB}}} \quad (II)$$

where  $Z$  is the collision frequency,  $E_a$  is the activation energy of the reaction (here:  $E_a = 0$ ),  $T$  is the temperature,  $R$  is gas constant,  $N_A$  is the Avogadro constant,  $\sigma_{AB} = \pi \cdot (r_{\text{HBr}} + r_{\text{Radical}})^2$  is the reaction cross section,  $k_B$  is the Boltzmann constant, and  $\mu_{AB} = (M_A + M_B) / M_A M_B$  is the reduced mass of the reactants. An *upper* limit to  $k_1$  is then given by:

$$k_1(T) = k_{1a}(T) + k_{1b}(T) = K_{1a}(T) \cdot k_{-1a}(T) + K_{1b}(T) \cdot k_{-1b}(T) \quad (III)$$

The equilibrium constants are related to Gibbs energy of reaction at STP:

$$\Delta G_T^\theta = -R \cdot T \cdot \ln(K^\theta(T)) \quad (IV)$$

Table 3.1 summarizes the molecular parameters employed in calculating the rate coefficients for the reverse reactions, and the calculated individual reverse and forward rate coefficients. For comparison, Table 3.2 shows the similarly derived results for the reaction of Br atoms with 2-aminoethanol (MEA). Finally, Table 3.3 compares the theoretical rate coefficients for Br atom reaction with methyl-, dimethyl- and trimethylamine, and 2-aminoethanol (MEA) with the rate coefficients for the corresponding OH radical and Cl atom reactions. For

methylamine the Br atom reaction is more than 2 orders of magnitude slower than the corresponding Cl atom reaction; for dimethylamine.

Table 3.1. Molecular parameters employed in calculating reaction rate coefficients from simple collision theory, and upper limits for rate coefficients at 298 K ( $\text{cm}^3 \text{ molecule}^{-1} \text{ s}^{-1}$ ) for reaction of HBr with aminoalkyl- and alkylamino radicals.

Parameter	HBr	$\text{CH}_3\text{NH}$	$\text{CH}_2\text{NH}_2$	$(\text{CH}_3)_2\text{N}$	$\text{CH}_3\text{NHCH}_2$	$(\text{CH}_3)_2\text{NCH}_2$
$r_x^a / 10^{-10} \text{ m}$	2.85	3.92	3.97	5.17	5.20	5.20
$m / 10^{-25} \text{ kg}$	1.344	4.990	4.990	7.319	7.319	9.648
$k_- (298 \text{ K})$		$7.72 \times 10^{-10}$	$7.84 \times 10^{-10}$	$9.50 \times 10^{-10}$	$9.57 \times 10^{-10}$	$8.79 \times 10^{-10}$
$\Delta G_{298}^\theta / \text{kJ mol}^{-1}$		40.3 <sup>b</sup>	14.4 <sup>b</sup>	12.3 <sup>b</sup>	10.4 <sup>b</sup>	6.1 <sup>b</sup>
$\square_{298}$		$8.63 \times 10^{-08}$	$2.99 \times 10^{-03}$	$6.98 \times 10^{-03}$	$1.50 \times 10^{-02}$	$8.53 \times 10^{-02}$
$k_+ (298 \text{ K})$		$6.66 \times 10^{-17}$	$2.34 \times 10^{-12}$	$6.63 \times 10^{-12}$	$1.44 \times 10^{-11}$	$7.49 \times 10^{-11}$

<sup>a</sup> Structure results from CCSD/aug-cc-pVDZ calculations. <sup>b</sup> Based on Gibbs energies from G4 calculations.

Table 3.2. Upper limits for rate coefficients at 298 K ( $\text{cm}^3 \text{ molecule}^{-1} \text{ s}^{-1}$ ) for reaction of HBr with  $\text{NH}_2\text{CH}_2\text{CH}_2\text{O}$ ,  $\text{NH}_2\text{CH}_2\text{CHOH}$ ,  $\text{NH}_2\text{CHCH}_2\text{OH}$  and  $\text{NHCH}_2\text{CH}_2\text{OH}$  radicals, and upper limits for rate coefficients at 298 K ( $\text{cm}^3 \text{ molecule}^{-1} \text{ s}^{-1}$ ) for reaction of HBr with aminoalkyl- and alkylamino radicals

Parameter	HBr	$\text{NH}_2\text{CH}_2\text{CH}_2\text{O}$	$\text{NH}_2\text{CH}_2\text{CHOH}$	$\text{NH}_2\text{CHCH}_2\text{OH}$	$\text{NHCH}_2\text{CH}_2\text{OH}$
$r_x^a / 10^{-10} \text{ m}$	2.85	5.15	5.20	5.10	5.10
$m / 10^{-25} \text{ kg}$	1.344	9.976	9.976	9.976	9.976
$k_- (298 \text{ K})$		$7.72 \times 10^{-10}$	$7.84 \times 10^{-10}$	$9.50 \times 10^{-10}$	$9.57 \times 10^{-10}$
$\Delta G_{298}^\theta / \text{kJ mol}^{-1}$		67.5 <sup>b</sup>	16.0 <sup>b</sup>	11.1 <sup>b</sup>	40.7 <sup>b</sup>
$\square_{298}$		$1.47 \times 10^{-12}$	$1.57 \times 10^{-03}$	$1.13 \times 10^{-02}$	$7.34 \times 10^{-08}$
$k_+ (298 \text{ K})$		$1.25 \times 10^{-21}$	$1.33 \times 10^{-12}$	$9.86 \times 10^{-12}$	$6.31 \times 10^{-17}$

<sup>a</sup> Structure results from CCSD/aug-cc-pVDZ calculations. <sup>b</sup> Based on Gibbs energies from G4 calculations.

Table 3.3. Experimental rate coefficients ( $\text{cm}^3 \text{ molecule}^{-1} \text{ s}^{-1}$ ) at 295-300 K for the reactions of amines with OH radicals and Cl atoms, and theoretically derived upper limit rate coefficients for amine reactions with Br atoms at 298 K.

Compound	$k_{\text{OH}} / 10^{-11}$	Ref.	$k_{\text{Cl}} / 10^{-10}$	Ref.	$k_{\text{Br}} / 10^{-11}$
CH <sub>3</sub> NH <sub>2</sub>	2.20 ± 0.22	36	3.5 ± 0.6	38	<0.23
	1.73 ± 0.11	37			
(CH <sub>3</sub> ) <sub>2</sub> NH	6.54 ± 0.66	39	3.9 <sup>+0.7</sup> <sub>-0.5</sub>	38	<2.1
	6.49 ± 0.64	37			
(CH <sub>3</sub> ) <sub>3</sub> N	6.09 ± 0.61	39	4.2 ± 0.5	38	<7.5
	3.58 ± 0.22	37			
	5.1 ± 0.5	40			
	3.24 ± 0.14	41			
NH <sub>2</sub> CH <sub>2</sub> CH <sub>2</sub> OH	9.2 ± 1.1	40			<1.1
	7.61 ± 0.76	41			

## 4 OH, CL AND BR CONCENTRATIONS IN THE MONGSTAD AREA

The Tel-Tek report no. 2211030-DC02, *Atmospheric Chemistry – Dark Chemistry. Nighttime Chemistry in the Mongstad Area: Literature Study and Model Simulations*, included a regional scale simulation of NO, NO<sub>2</sub>, NO<sub>3</sub>, O<sub>3</sub>, OH and several other species for the year 2006.<sup>42</sup> Figure 4.1 shows the simulated OH concentration in the Mongstad area during 2006; the average OH concentration is  $9.6 \times 10^5 \text{ cm}^{-3}$ .

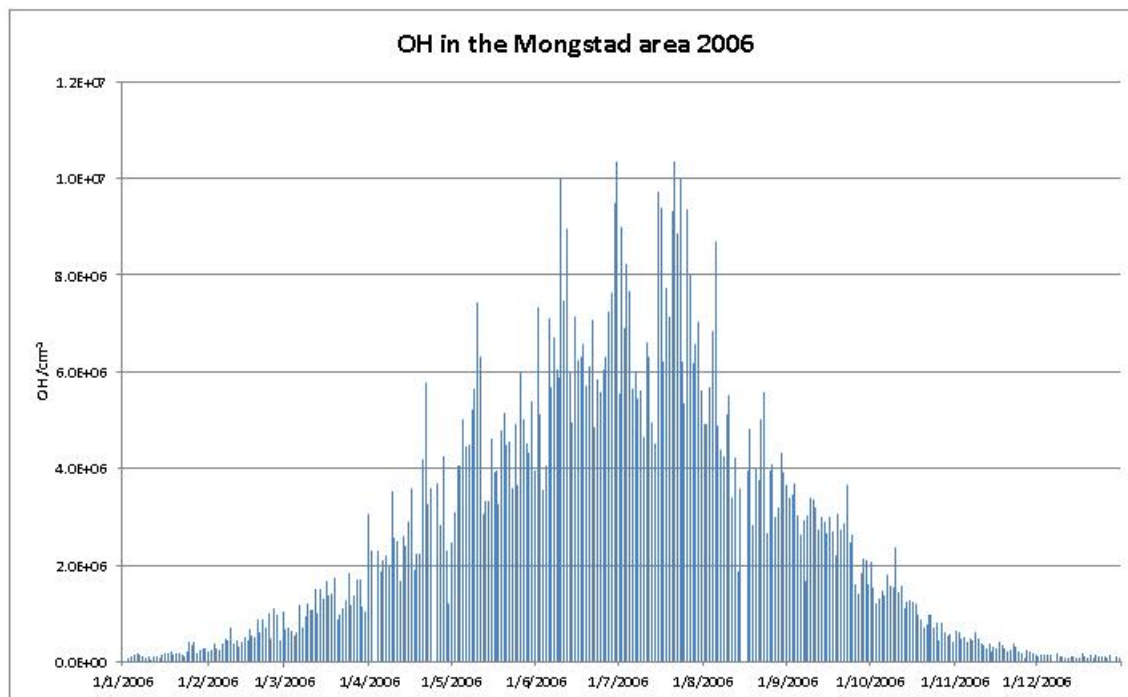


Figure 4.1. Model simulation of the OH concentration in the Mongstad area 2006. Data from Ref. 42.

Figure 4.2 shows the results from a marine-urban scenario simulation of the Cl concentration in the Mongstad area at Winter Solstice, Spring Equinox and Summer Solstice.<sup>1</sup> According to the marine-urban scenario model results, the average Cl concentration through the year should be around  $2 \times 10^3 \text{ cm}^{-3}$  in the Mongstad area.

The modelled time-profile for Br atom concentration in a mixed marine-urban scenario (Figure 3 in the Tel-Tek report no. 2211030-CC02, *Halogen Chemistry in the Mongstad Region: Literature Study and Model Simulations*<sup>1</sup>) is reproduced in Figure 4.3 (no data for the Spring Equinox were given). It was stated that the expected Br atom concentration could be 1-2 orders of magnitude larger than those in the figure.

The Br atom time profiles for the Winter and Summer Solstice resemble those of the Cl atom, and, assuming that the seasonal variation of the Br atoms concentration follow that of the Cl atom, the Spring Equinox Br atom concentration was obtained by scaling the model results from the Cl atoms concentration. It is believed that any error arising from this approximation will be small compared to the general model uncertainty. The upscaled Br atom concentration time-profiles for Winter Solstice, Spring Equinox and Summer Solstice are presented in Figure 4.4. Taking the yearly average Br gas phase concentration to be the same as that of the Spring Equinox results in an annual average Br atom concentration of  $3.6 \times 10^5 \text{ cm}^{-3}$  in the Mongstad area.

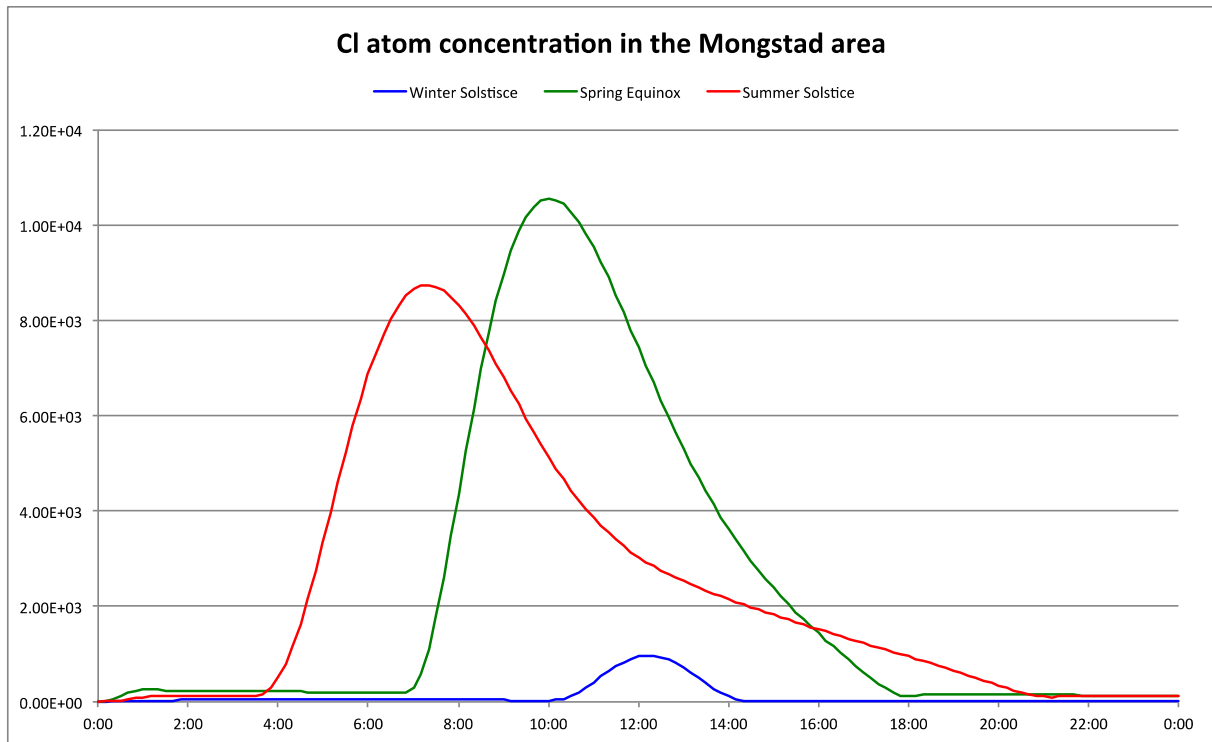


Figure 4.2. Simulated concentration (cm<sup>-3</sup>) of gas phase Cl atoms in the Mongstad area 2006. Results from mixed marine-urban scenario. Data from Ref. 1.

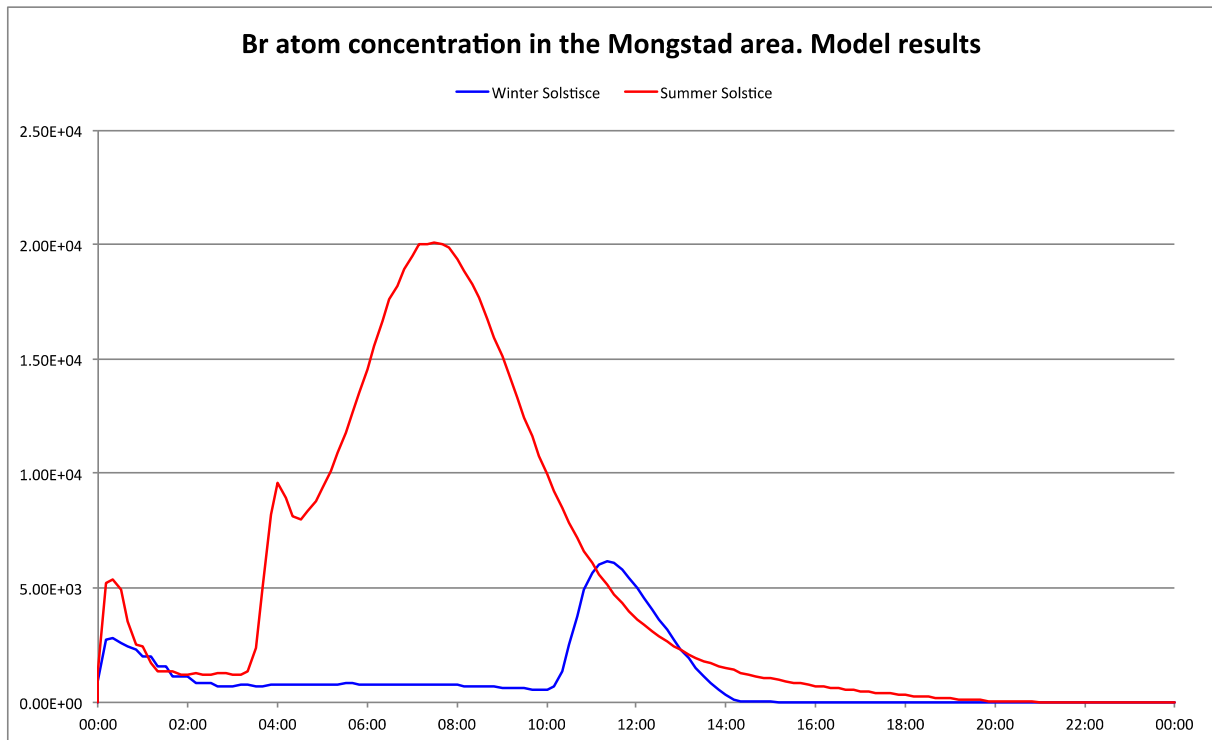


Figure 4.3. Simulated concentration (cm<sup>-3</sup>) of gas phase Br atoms in the Mongstad area 2006. Results from mixed marine-urban scenario. Data from Ref. 1.

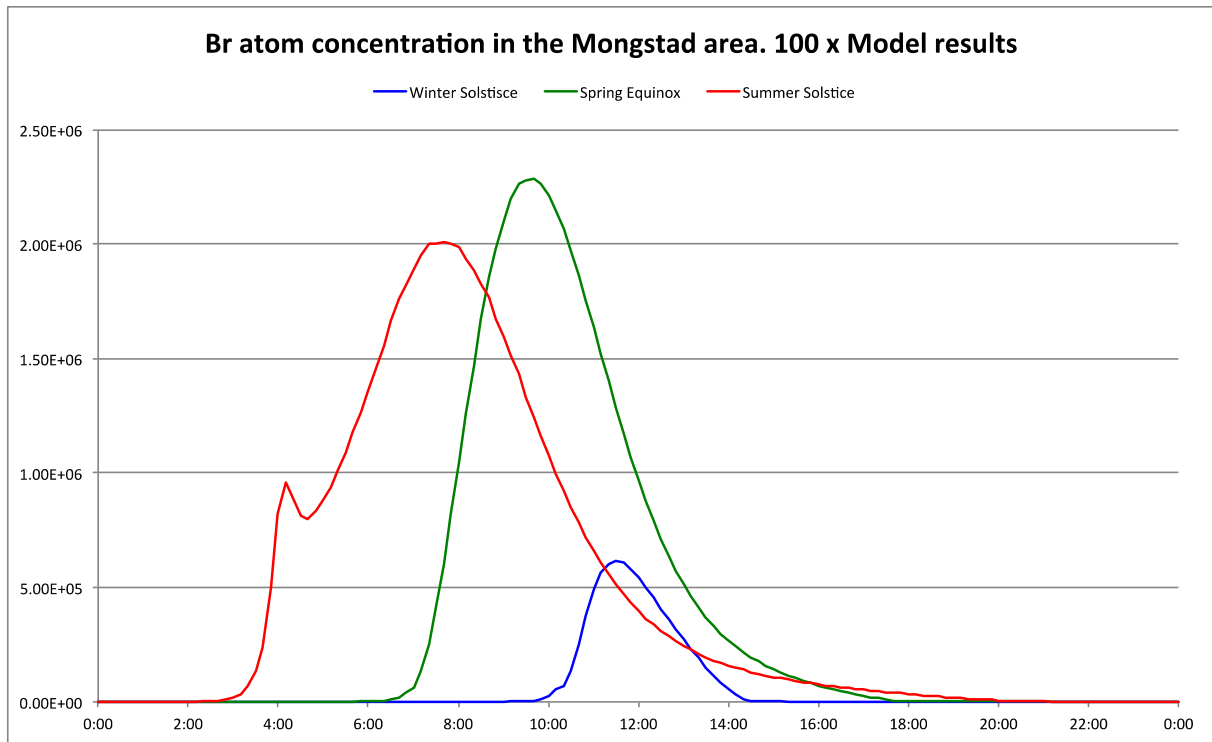


Figure 4.4. Simulated concentration ( $\text{cm}^{-3}$ ) of gas phase Br atoms in the Mongstad area 2006. Results from scaling of mixed marine-urban scenario by 100. Data based on results presented in Ref. 1.

## 5 BOX MODEL CALCULATIONS OF AMINE + OH, CL AND BR REACTIONS

The objective is to evaluate the relative importance of gas phase removal by Cl, Br and OH radicals in the Mongstad area. Experimental rate coefficients for Cl atom and OH radical reaction with methyl-, dimethyl- and trimethylamine have been reported, while only upper limits to the Br atom reactions with the same amines are available from the present theoretical study, Table 3.3.

Although the seasonal variations may differ from year to year there is no reason to expect average values of OH, Cl and Br to be different in 2006 from other years. Consequently, the average lifetimes of an amine with respect to reaction with OH, Cl and Br in the Mongstad area may be estimated to be  $\tau_{OH} = (k_{OH} \cdot \langle [OH] \rangle_{year})^{-1}$ ,  $\tau_{Cl} = (k_{Cl} \cdot \langle [Cl] \rangle_{year})^{-1}$  and  $\tau_{Br} = (k_{Br} \cdot \langle [Br] \rangle_{year})^{-1}$ . Table 5.1 shows the estimated atmospheric gas phase lifetimes of methyl-, dimethyl, trimethylamine and MEA with respect to reaction with OH, Cl and Br.

Table 5.1. Rate coefficients ( $\text{cm}^3 \text{ molecule}^{-1} \text{ s}^{-1}$ ) and estimated atmospheric lifetimes of amines with respect to reaction with OH, Cl and Br in the Mongstad area.

Amine	$k_{OH}$	$\tau_{OH}^a$	$k_{Cl}$	$\tau_{Cl}^b$	$k_{Br}$	$\tau_{Br}^c$
$\text{CH}_3\text{NH}_2$	$2 \times 10^{-11}$	14 h	$3.5 \times 10^{-10}$	16 d	$< 0.23 \times 10^{-11}$	> 14 d
$(\text{CH}_3)_2\text{NH}$	$6.5 \times 10^{-11}$	4 ½ h	$3.9 \times 10^{-10}$	15 d	$< 2.1 \times 10^{-11}$	> 1½ d
$(\text{CH}_3)_3\text{N}$	$5 \times 10^{-11}$	6 h	$4.2 \times 10^{-10}$	14 d	$< 7.5 \times 10^{-11}$	> 10 h
$\text{NH}_2\text{CH}_2\text{CH}_2\text{OH}$	$7.6 \times 10^{-11}$	3 h		No data	$< 1.1 \times 10^{-11}$	> 3 d

<sup>a</sup>  $[\text{OH}]_a = 9.6 \times 10^5 \text{ cm}^{-3}$ ; <sup>b</sup>  $[\text{Cl}]_a = 2 \times 10^3 \text{ cm}^{-3}$ ; <sup>c</sup>  $[\text{Br}]_a = 3.6 \times 10^5 \text{ cm}^{-3}$ .

It can be seen from Table 5.1 that the atmospheric amine loss due to reaction with Br atoms may actually be larger than that due to reaction with Cl atoms. With the exception of trimethylamine (and likely also other tertiary amines) the dominant atmospheric amine loss is due to reaction with OH radicals. Seasonal variations are illustrated in sections 5.1 through 5.3 without comments. The results are based on the modelled time-profile for Br atom concentration in a mixed marine-urban scenario.<sup>1</sup> Results for three Br atom concentration scenarios are presented:

1. The simulated seasonal Br atom concentration;  $[\text{Br}]_a = 3.6 \times 10^3 \text{ cm}^{-3}$ .
2. The simulated seasonal Br atom concentration increased by one order of magnitude;  $[\text{Br}]_a = 3.6 \times 10^4 \text{ cm}^{-3}$ .
3. The simulated seasonal Br atom concentration increased by two orders of magnitude (see Figure 4.4);  $[\text{Br}]_a = 3.6 \times 10^5 \text{ cm}^{-3}$ .

## 5.1 Model results for the period around Winter Solstice

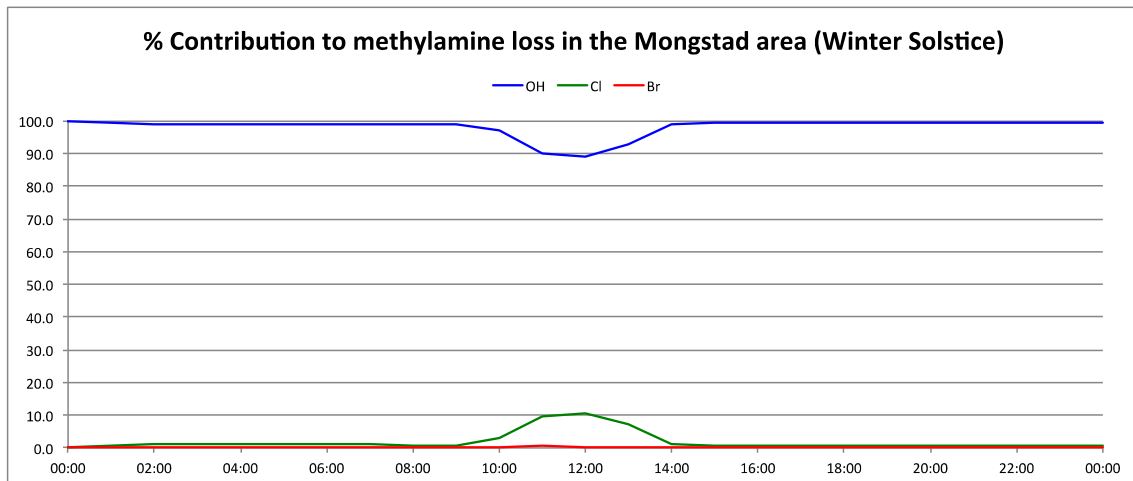


Figure 5.1. Box model results for methylamine gas phase loss due to reaction with OH radicals, and Cl and Br atoms in the Mongstad area around Winter Solstice.

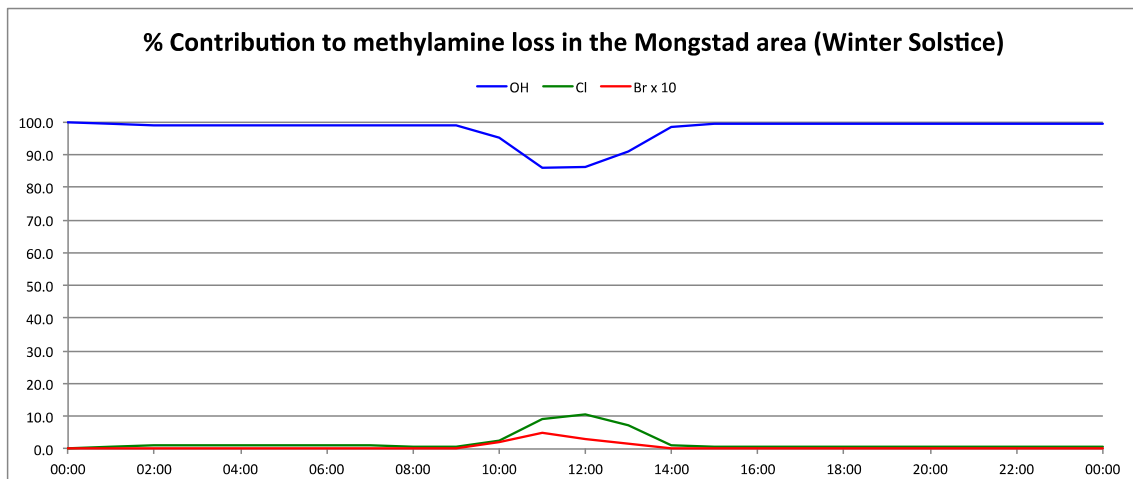


Figure 5.2. Box model results for methylamine gas phase loss due to reaction with OH radicals, and Cl and Br atoms in the Mongstad area around Winter Solstice. Br concentration enhanced by a factor of 10.

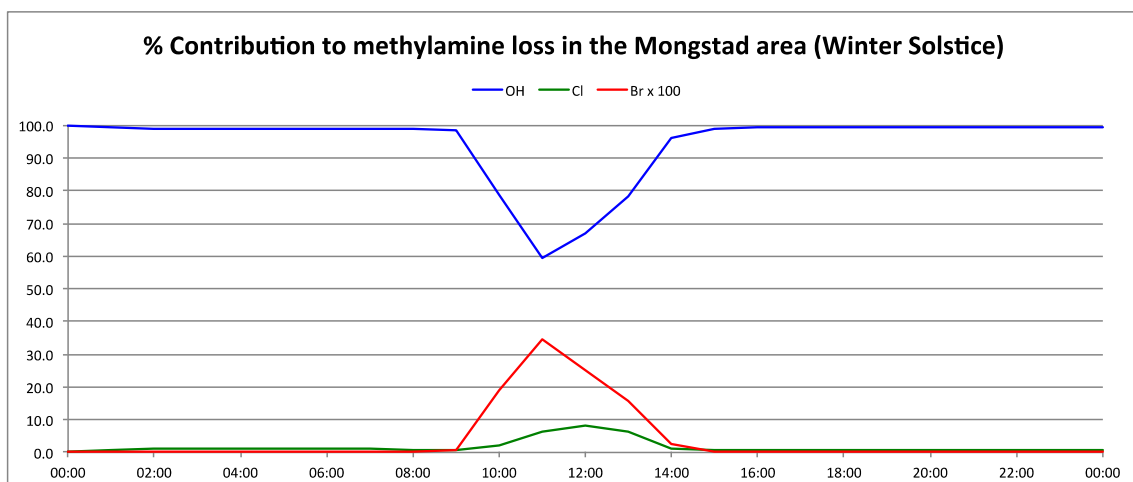


Figure 5.3. Box model results for methylamine gas phase loss due to reaction with OH radicals, and Cl and Br atoms in the Mongstad area around Winter Solstice. Br concentration enhanced by a factor of 100.

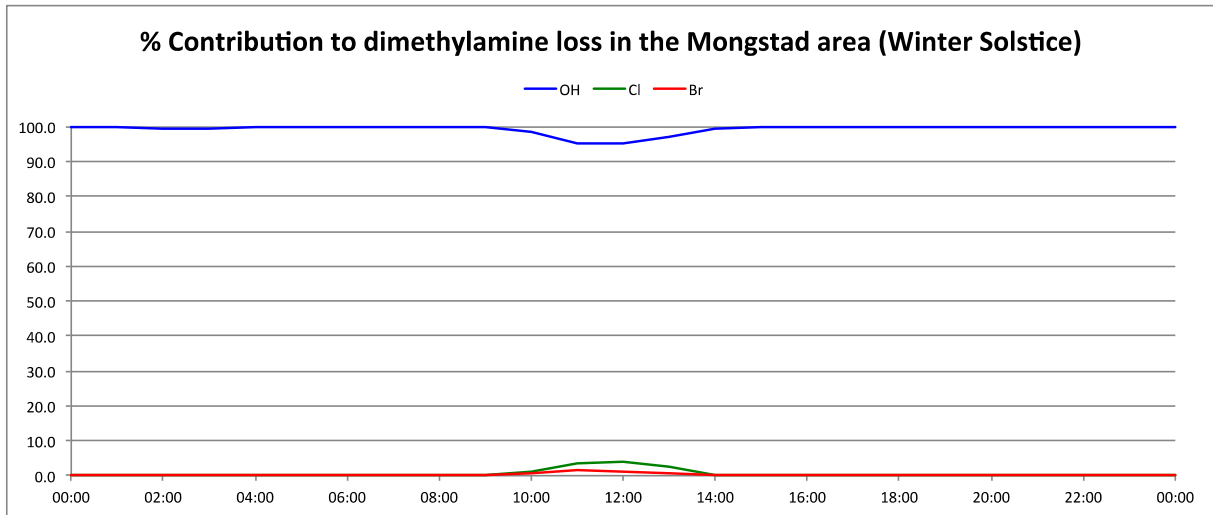


Figure 5.4. Box model results for dimethylamine gas phase loss due to reaction with OH radicals, and Cl and Br atoms in the Mongstad area around Winter Solstice.

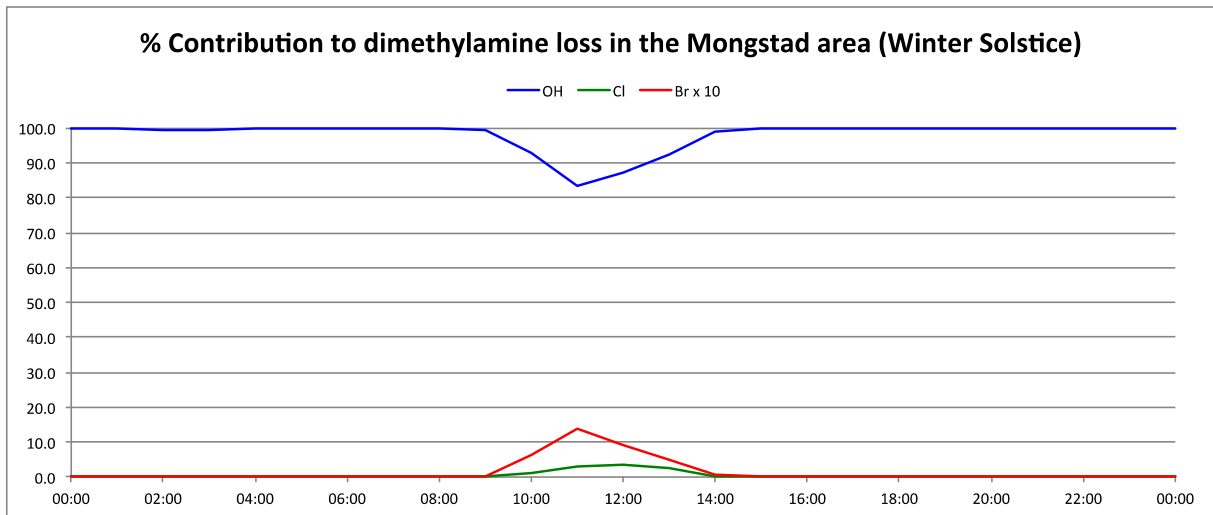


Figure 5.5. Box model results for dimethylamine gas phase loss due to reaction with OH radicals, and Cl and Br atoms in the Mongstad area around Winter Solstice. Br concentration enhanced by a factor of 10.

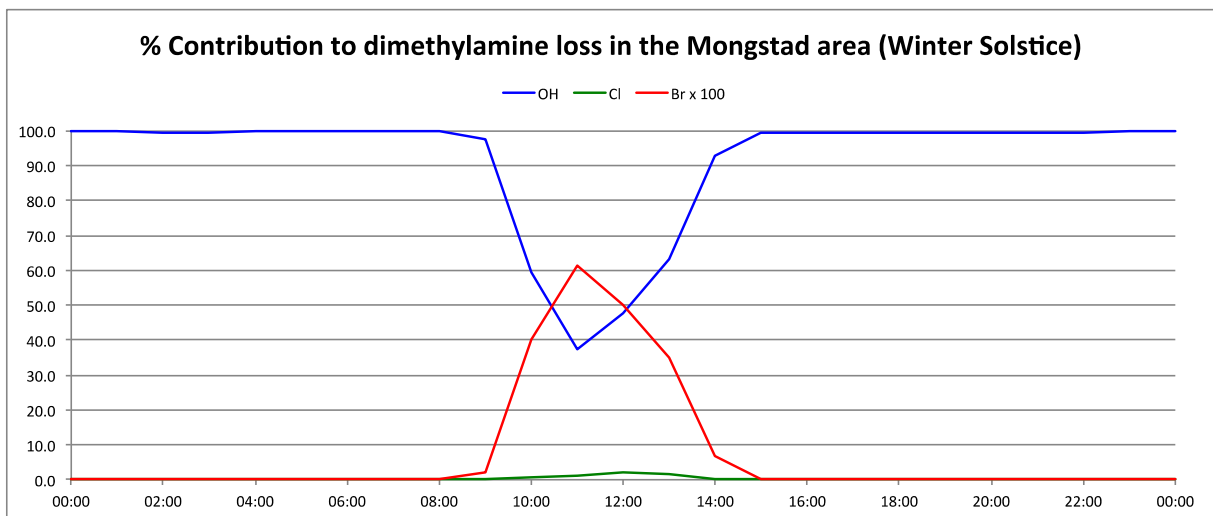


Figure 5.6. Box model results for dimethylamine gas phase loss due to reaction with OH radicals, and Cl and Br atoms in the Mongstad area around Winter Solstice. Br concentration enhanced by a factor of 100.

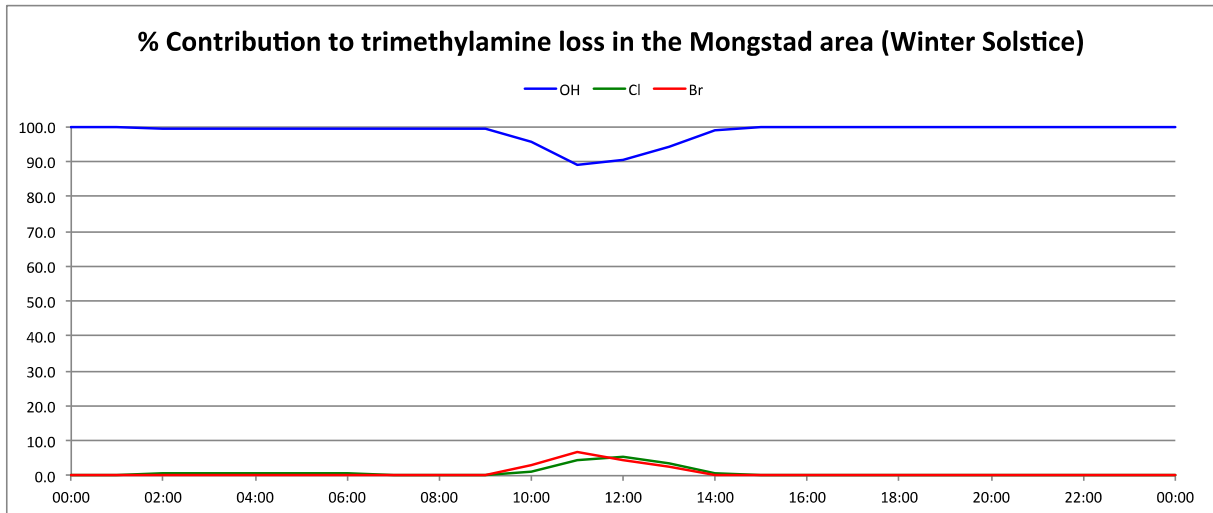


Figure 5.7. Box model results for trimethylamine gas phase loss due to reaction with OH radicals, and Cl and Br atoms in the Mongstad area around Winter Solstice.

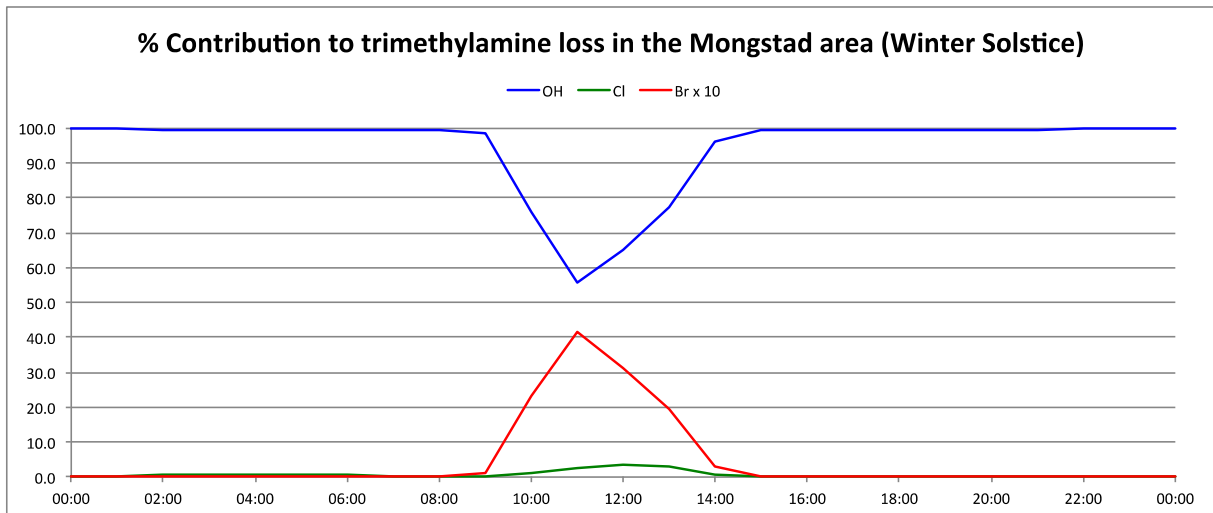


Figure 5.8. Box model results for trimethylamine gas phase loss due to reaction with OH radicals, and Cl and Br atoms in the Mongstad area around Winter Solstice. Br concentration enhanced by a factor of 10.

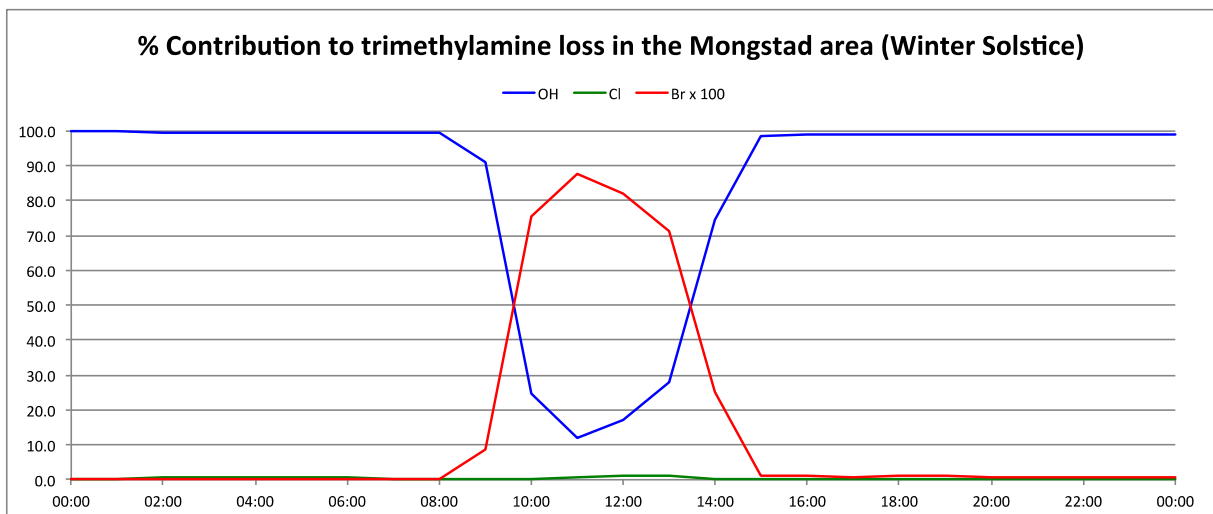


Figure 5.9. Box model results for trimethylamine gas phase loss due to reaction with OH radicals, and Cl and Br atoms in the Mongstad area around Winter Solstice. Br concentration enhanced by a factor of 100.

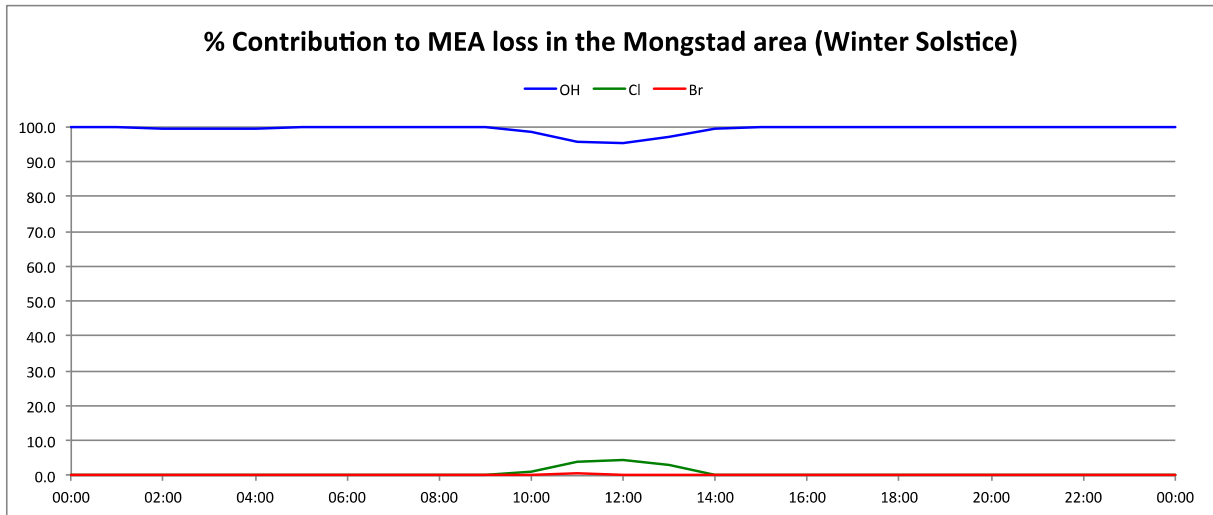


Figure 5.10. Box model results for 2-aminoethanol (MEA) gas phase loss due to reaction with OH radicals, and Cl and Br atoms in the Mongstad area around Winter Solstice.

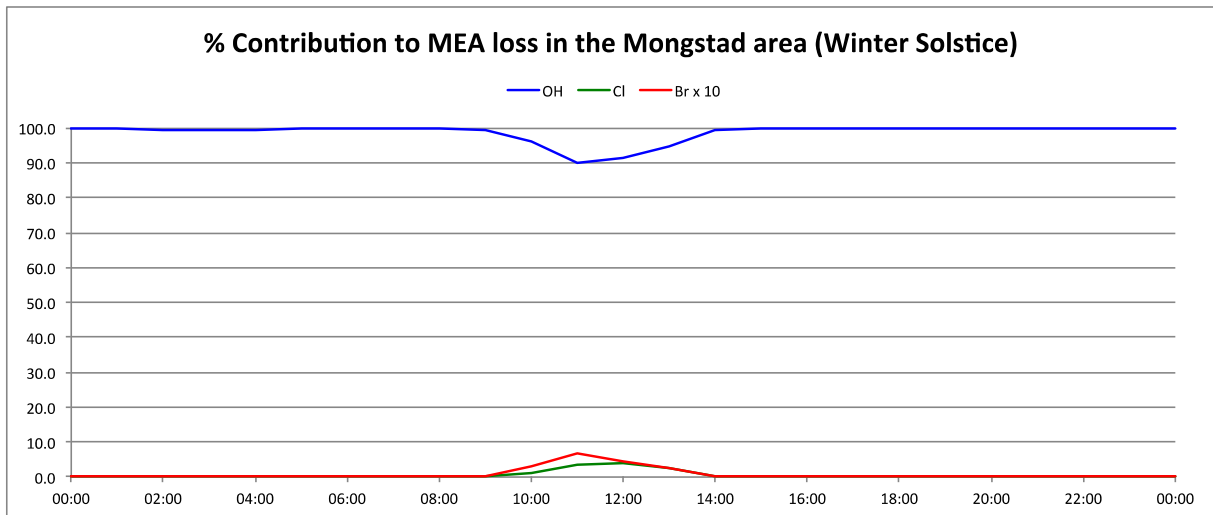


Figure 5.11. Box model results for 2-aminoethanol (MEA) gas phase loss due to reaction with OH radicals, and Cl and Br atoms in the Mongstad area around Winter Solstice. Br concentration enhanced by a factor of 10.

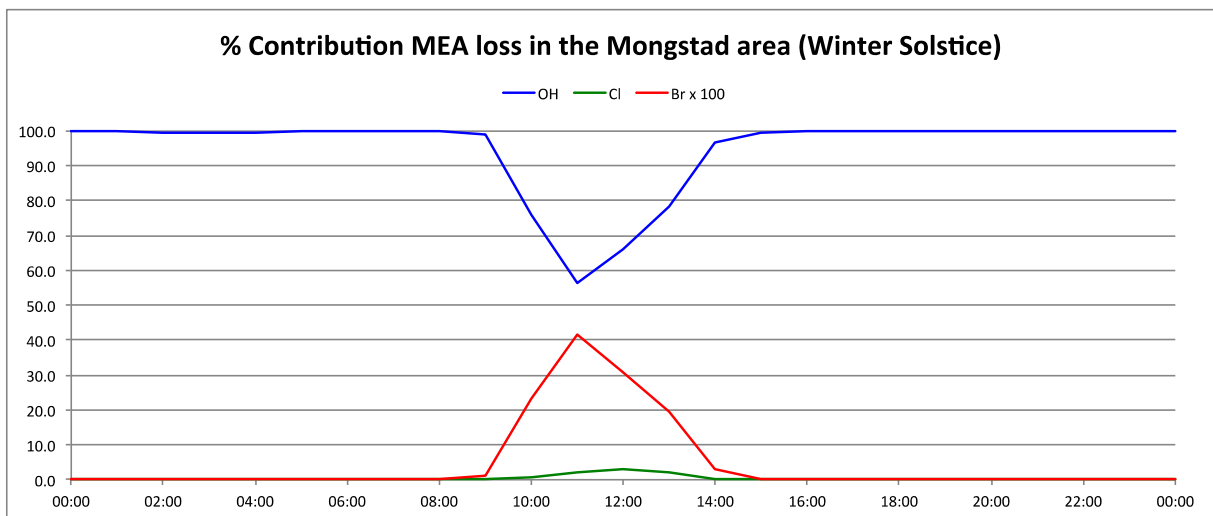


Figure 5.12. Box model results for 2-aminoethanol (MEA) gas phase loss due to reaction with OH radicals, and Cl and Br atoms in the Mongstad area around Winter Solstice. Br concentration enhanced by a factor of 100.

## 5.2 Model results for the period around Spring Equinox

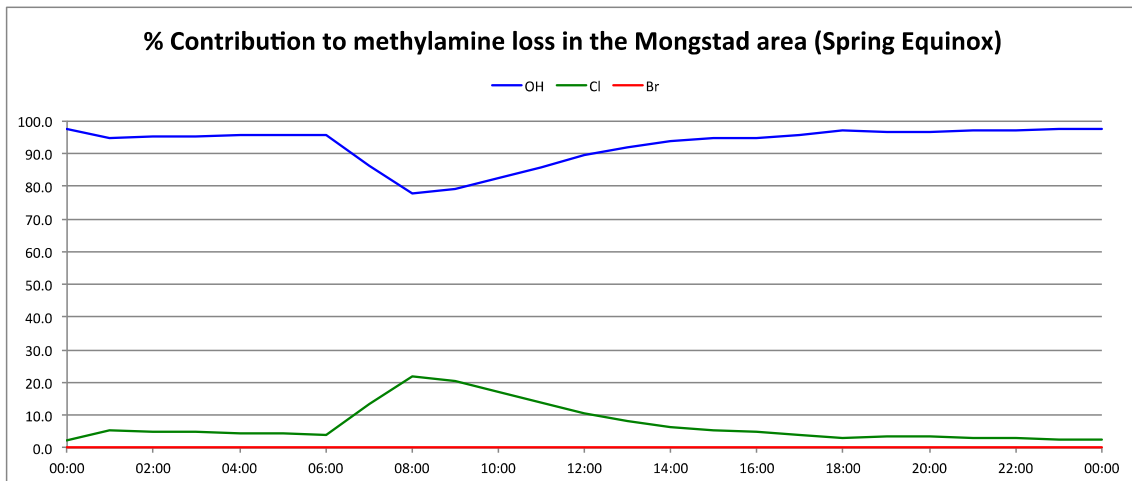


Figure 5.13. Box model results for methylamine gas phase loss due to reaction with OH radicals, and Cl and Br atoms in the Mongstad area around Spring Equinox.

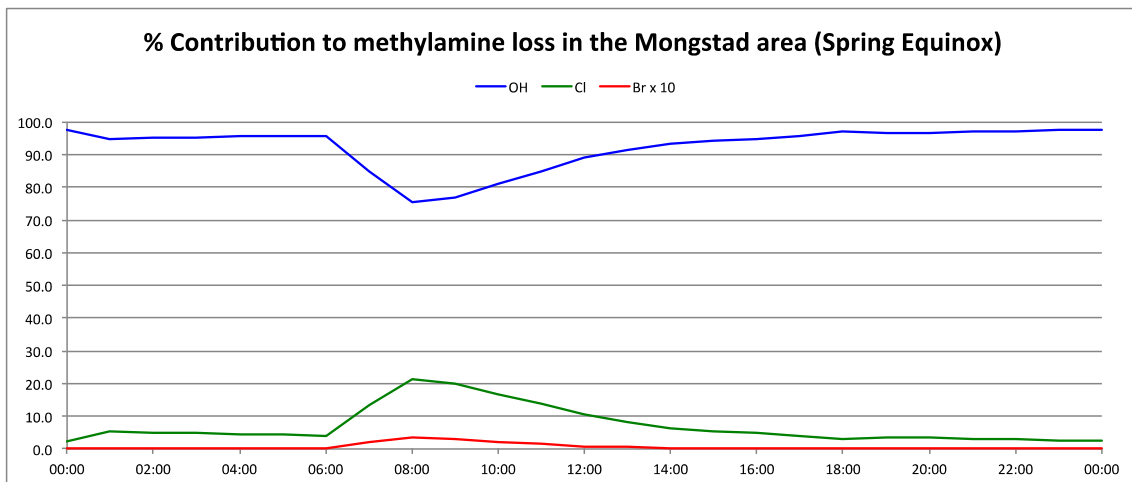


Figure 5.14. Box model results for methylamine gas phase loss due to reaction with OH radicals, and Cl and Br atoms in the Mongstad area around Spring Equinox. Br concentration enhanced by a factor of 10.

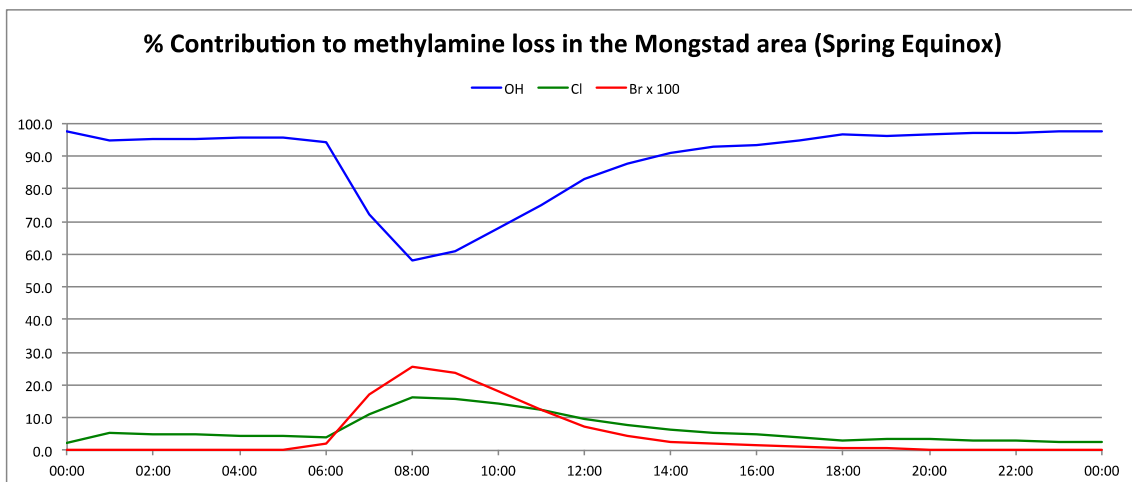


Figure 5.15. Box model results for methylamine gas phase loss due to reaction with OH radicals, and Cl and Br atoms in the Mongstad area around Spring Equinox. Br concentration enhanced by a factor of 100.

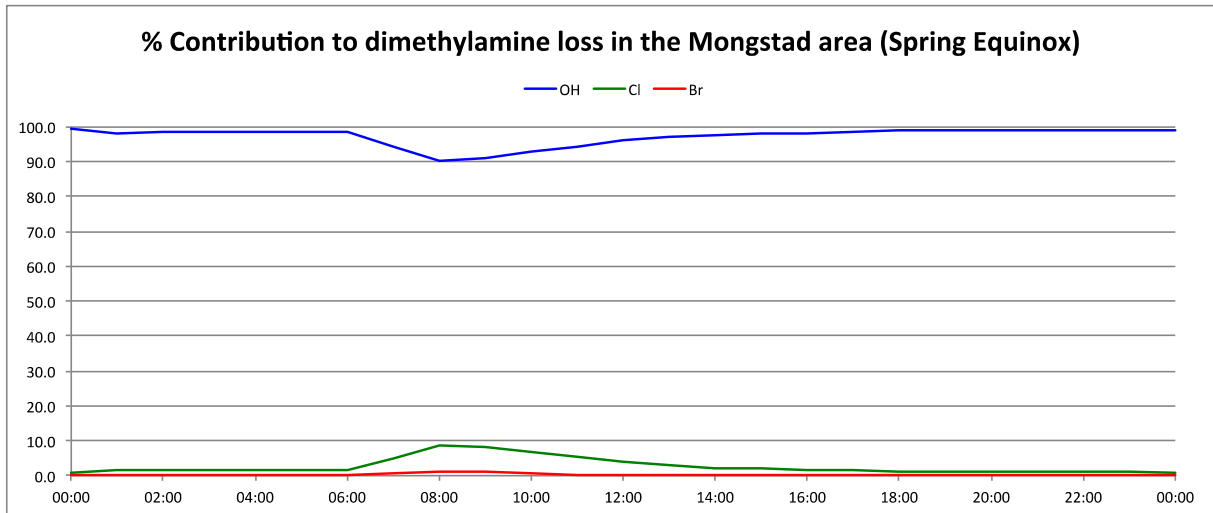


Figure 5.16. Box model results for dimethylamine gas phase loss due to reaction with OH radicals, and Cl and Br atoms in the Mongstad area around Spring Equinox.

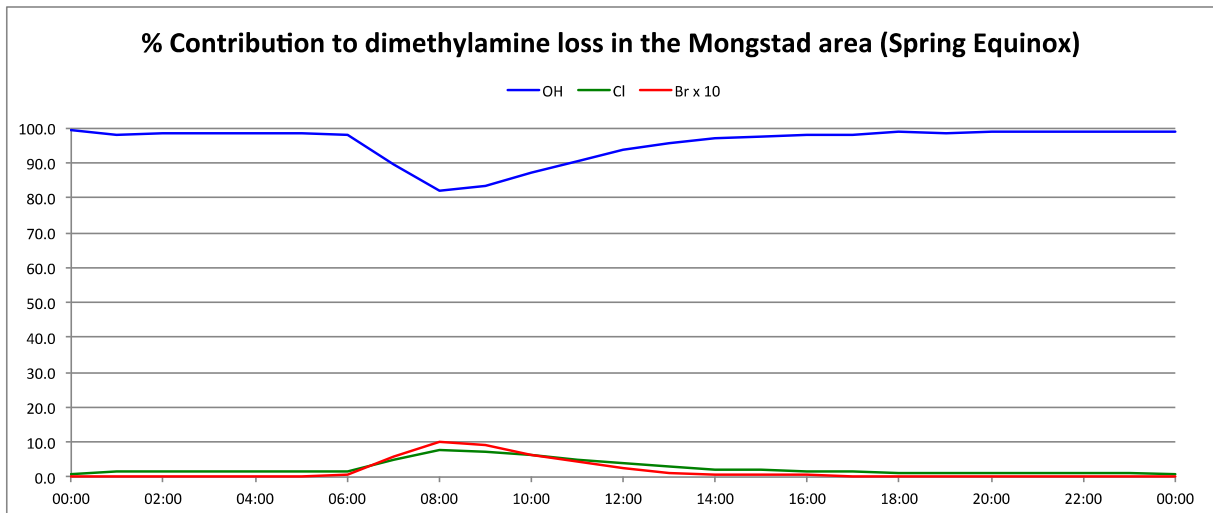


Figure 5.17. Box model results for dimethylamine gas phase loss due to reaction with OH radicals, and Cl and Br atoms in the Mongstad area around Spring Equinox. Br concentration enhanced by a factor of 10.

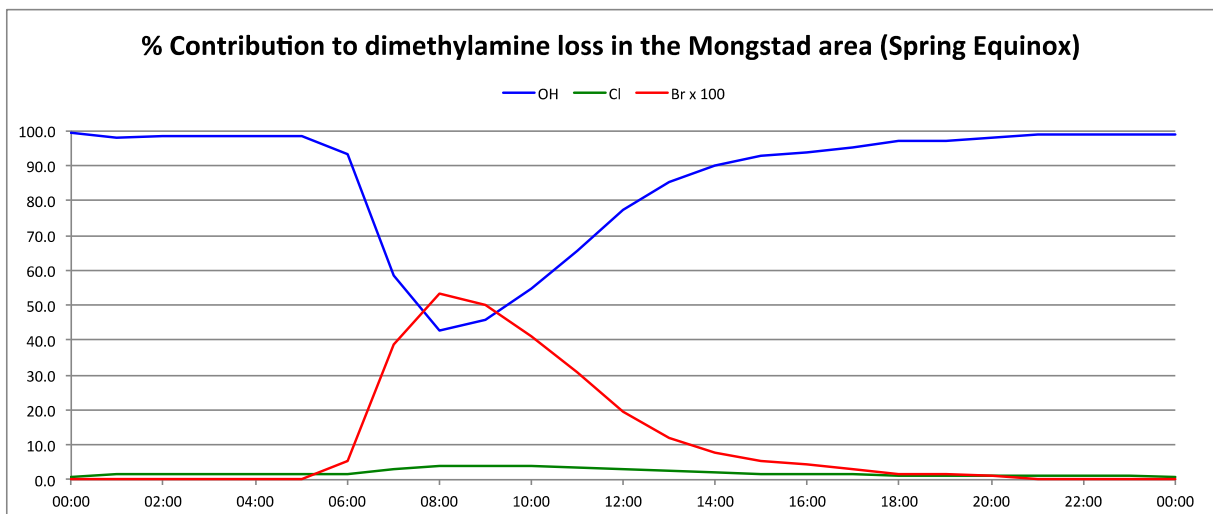


Figure 5.18. Box model results for dimethylamine gas phase loss due to reaction with OH radicals, and Cl and Br atoms in the Mongstad area around Spring Equinox. Br concentration enhanced by a factor of 100.

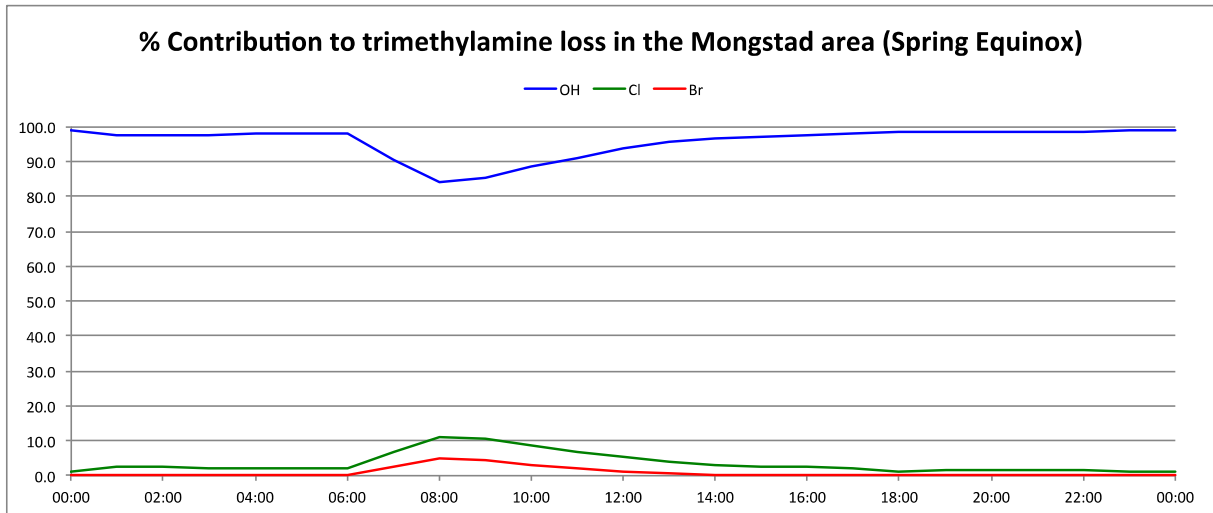


Figure 5.19. Box model results for trimethylamine gas phase loss due to reaction with OH radicals, and Cl and Br atoms in the Mongstad area around Spring Equinox.

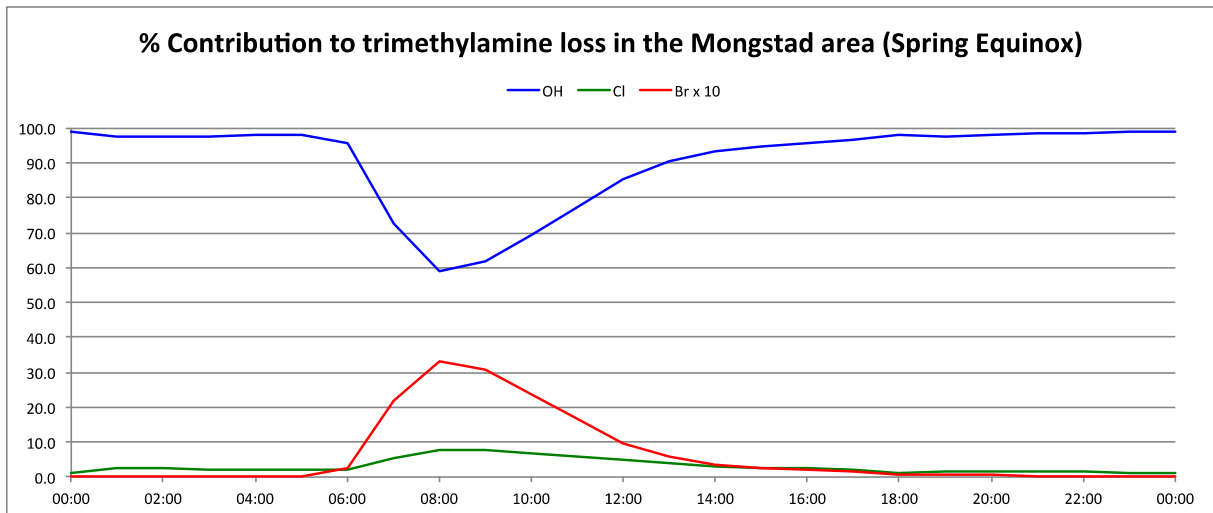


Figure 5.20. Box model results for trimethylamine gas phase loss due to reaction with OH radicals, and Cl and Br atoms in the Mongstad area around Spring Equinox. Br concentration enhanced by a factor of 10.

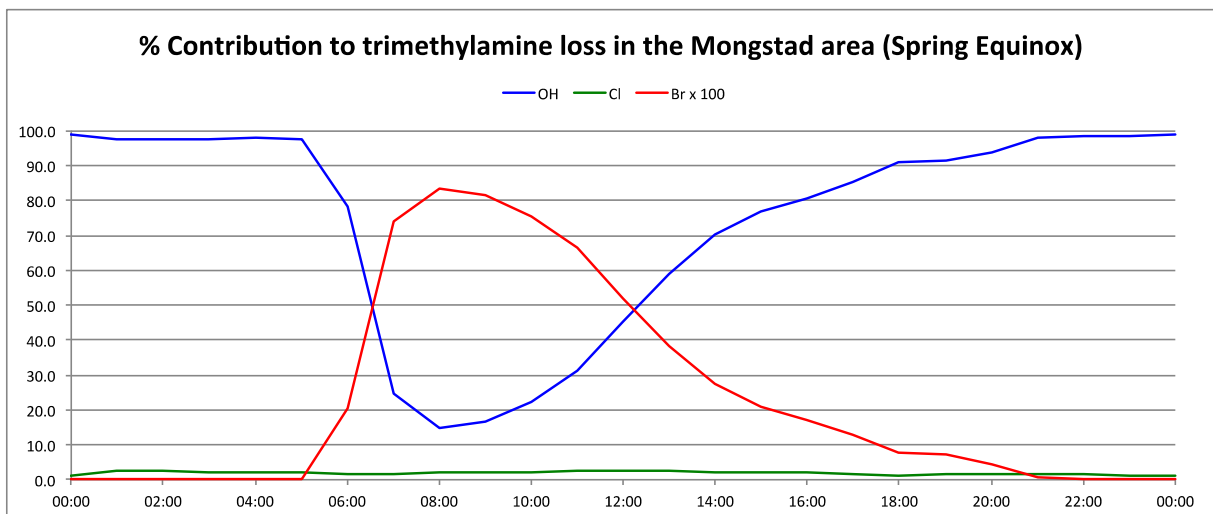


Figure 5.21. Box model results for trimethylamine gas phase loss due to reaction with OH radicals, and Cl and Br atoms in the Mongstad area around Spring Equinox. Br concentration enhanced by a factor of 100.

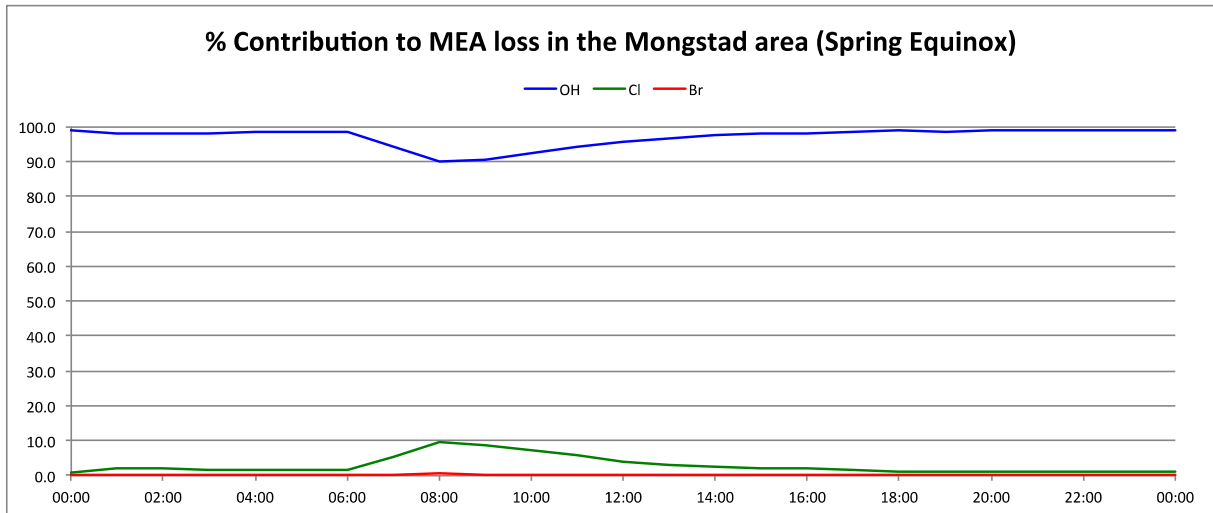


Figure 5.22. Box model results for 2-aminoethanol (MEA) gas phase loss due to reaction with OH radicals, and Cl and Br atoms in the Mongstad area around Spring Equinox.

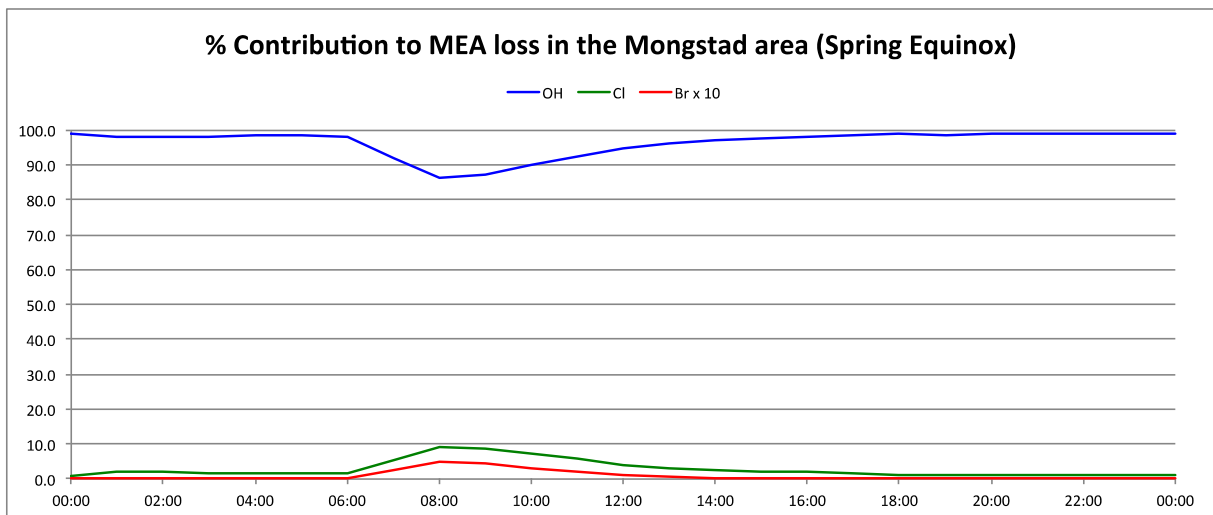


Figure 5.23. Box model results for 2-aminoethanol (MEA) gas phase loss due to reaction with OH radicals, and Cl and Br atoms in the Mongstad area around Spring Equinox. Br concentration enhanced by a factor of 10.

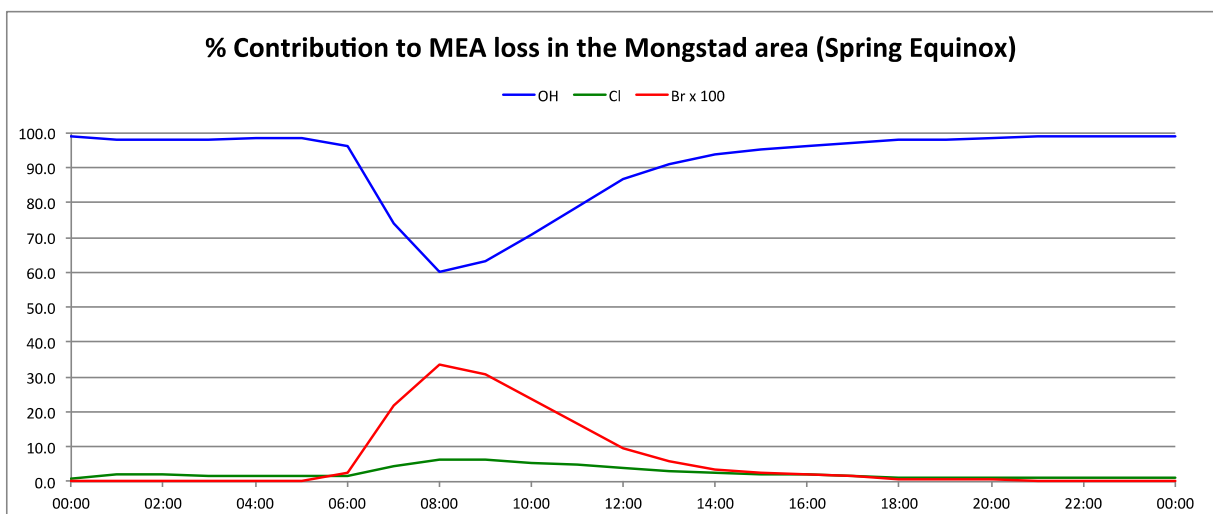


Figure 5.24. Box model results for 2-aminoethanol (MEA) gas phase loss due to reaction with OH radicals, and Cl and Br atoms in the Mongstad area around Spring Equinox. Br concentration enhanced by a factor of 100.

### 5.3 Model results for the period around Summer Solstice

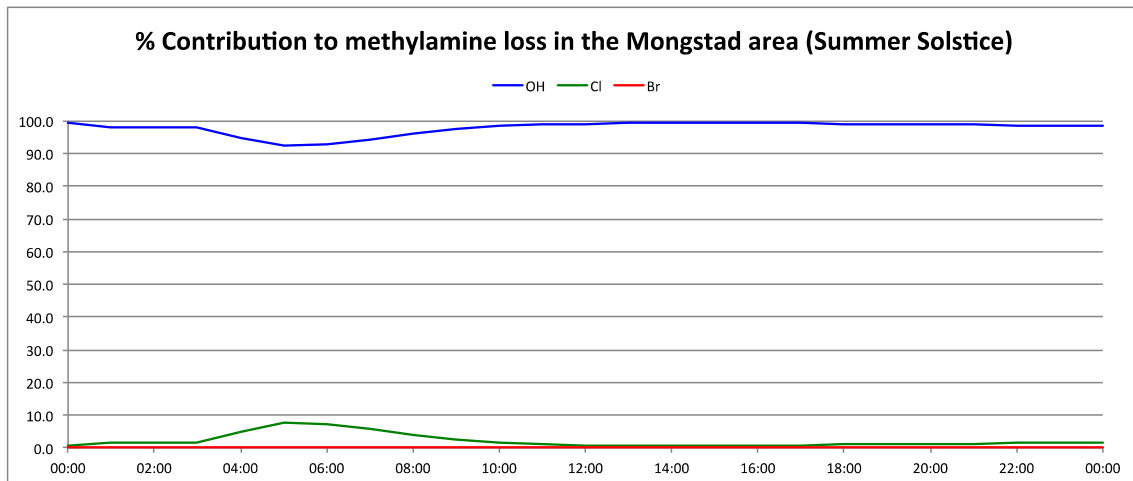


Figure 5.25. Box model results for methylamine gas phase loss due to reaction with OH radicals, and Cl and Br atoms in the Mongstad area around Summer Solstice.

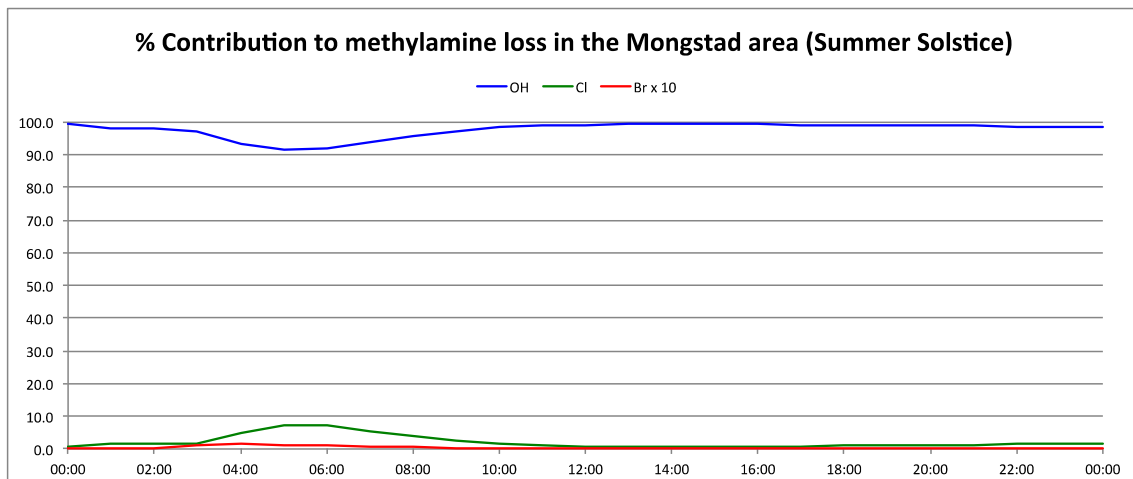


Figure 5.26. Box model results for methylamine gas phase loss due to reaction with OH radicals, and Cl and Br atoms in the Mongstad area around Summer Solstice. Br concentration enhanced by a factor of 10.

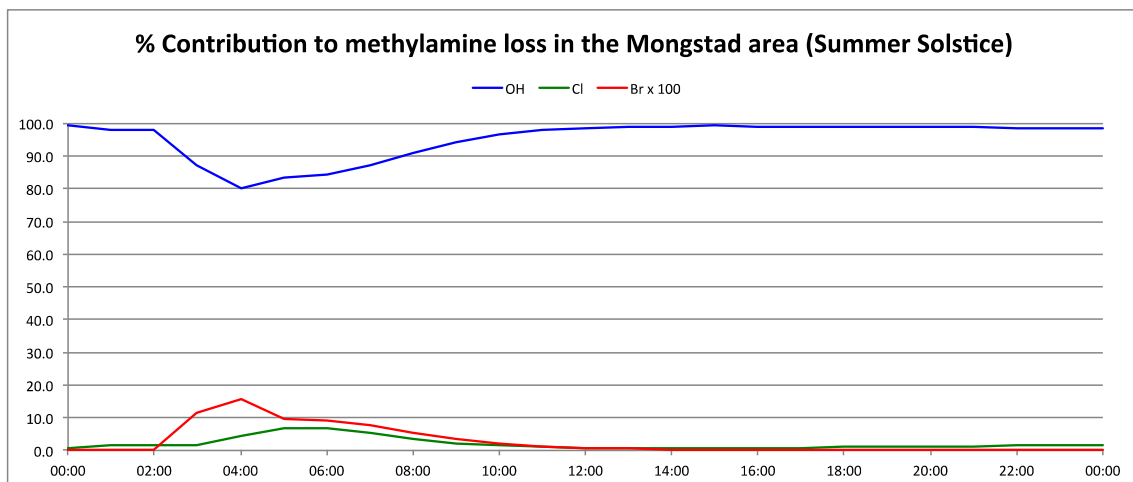


Figure 5.27. Box model results for methylamine gas phase loss due to reaction with OH radicals, and Cl and Br atoms in the Mongstad area around Summer Solstice. Br concentration enhanced by a factor of 100.

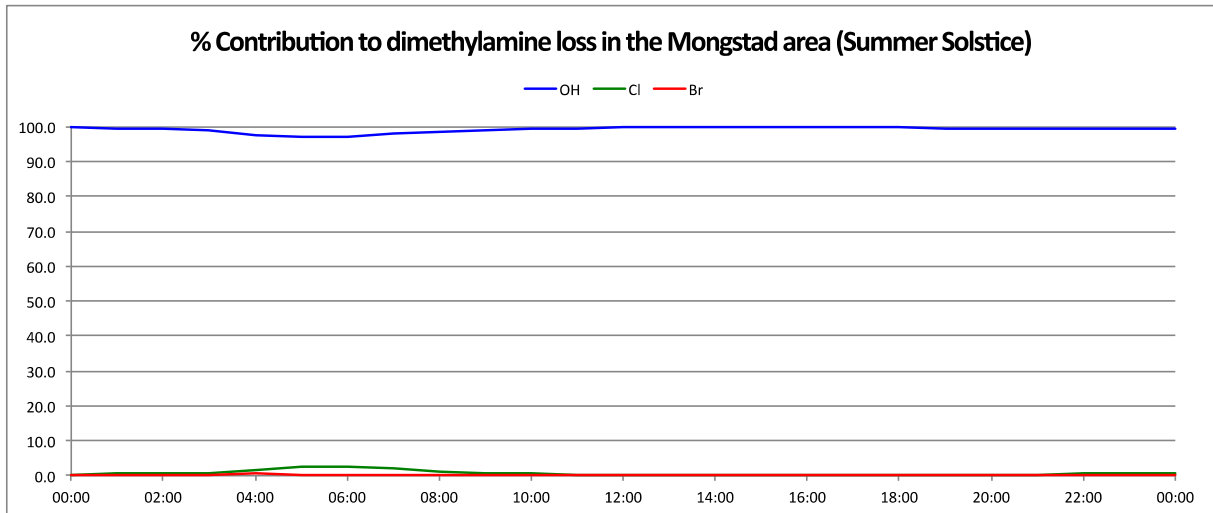


Figure 5.28. Box model results for dimethylamine gas phase loss due to reaction with OH radicals, and Cl and Br atoms in the Mongstad area around Summer Solstice.

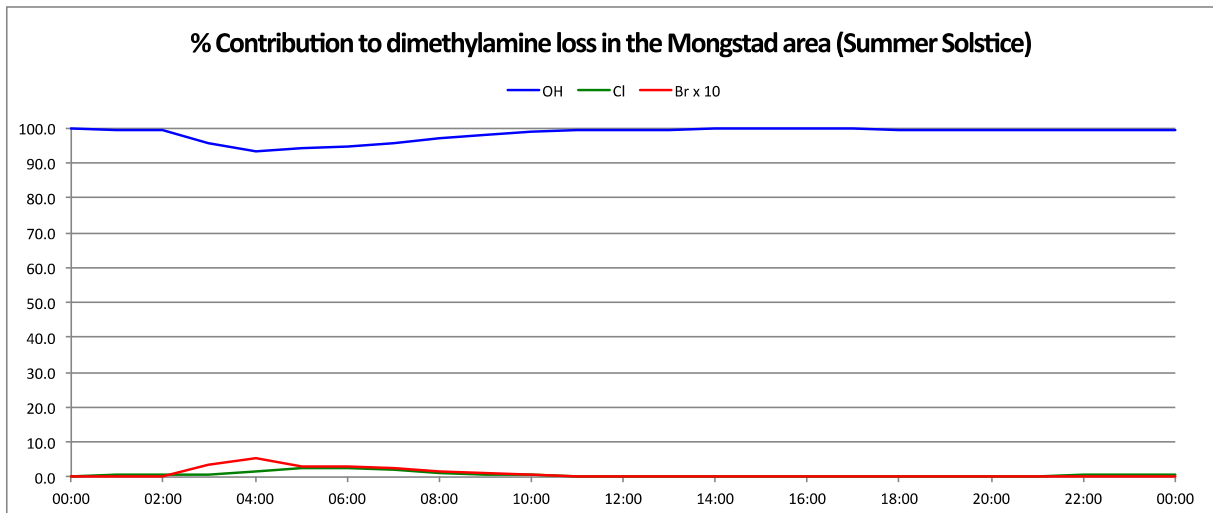


Figure 5.29. Box model results for dimethylamine gas phase loss due to reaction with OH radicals, and Cl and Br atoms in the Mongstad area around Summer Solstice. Br concentration enhanced by a factor of 10.

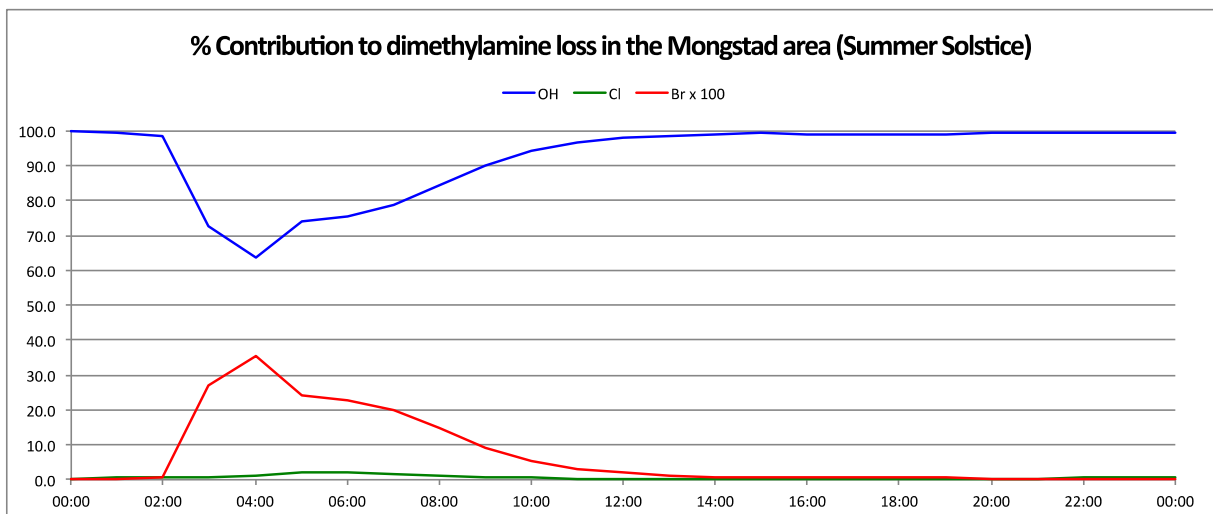


Figure 5.30. Box model results for dimethylamine gas phase loss due to reaction with OH radicals, and Cl and Br atoms in the Mongstad area around Summer Solstice. Br concentration enhanced by a factor of 100.

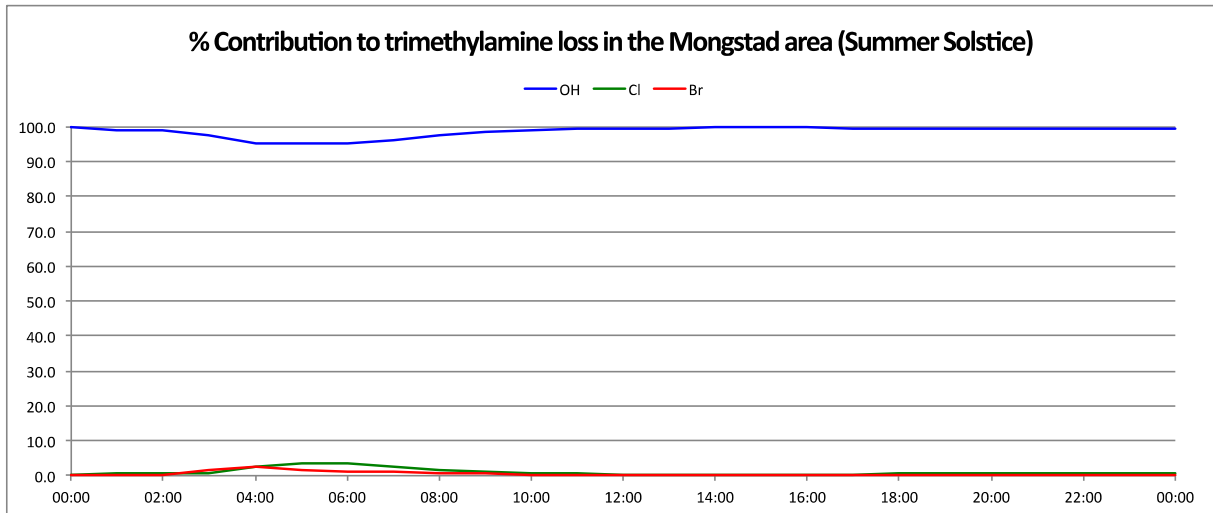


Figure 5.31. Box model results for trimethylamine gas phase loss due to reaction with OH radicals, and Cl and Br atoms in the Mongstad area around Summer Solstice.

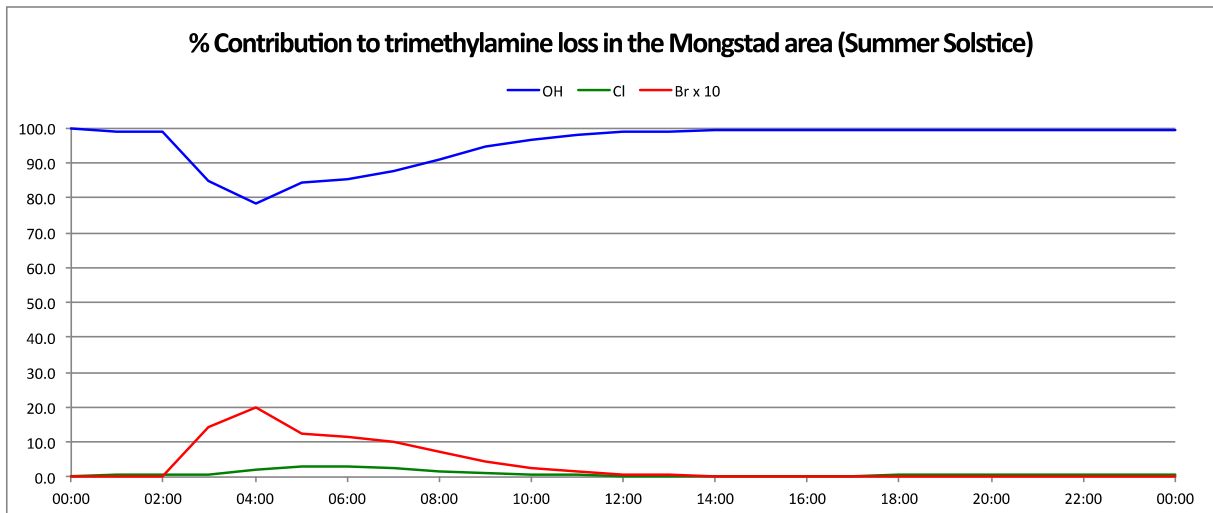


Figure 5.32. Box model results for trimethylamine gas phase loss due to reaction with OH radicals, and Cl and Br atoms in the Mongstad area around Summer Solstice. Br concentration enhanced by a factor of 10.

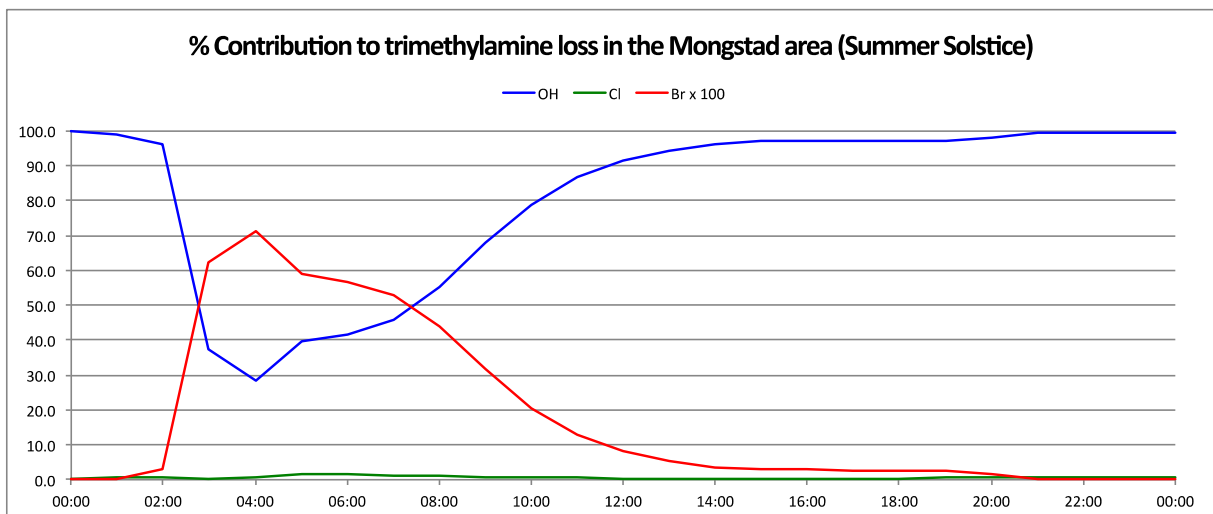


Figure 5.33. Box model results for trimethylamine gas phase loss due to reaction with OH radicals, and Cl and Br atoms in the Mongstad area around Summer Solstice. Br concentration enhanced by a factor of 100.

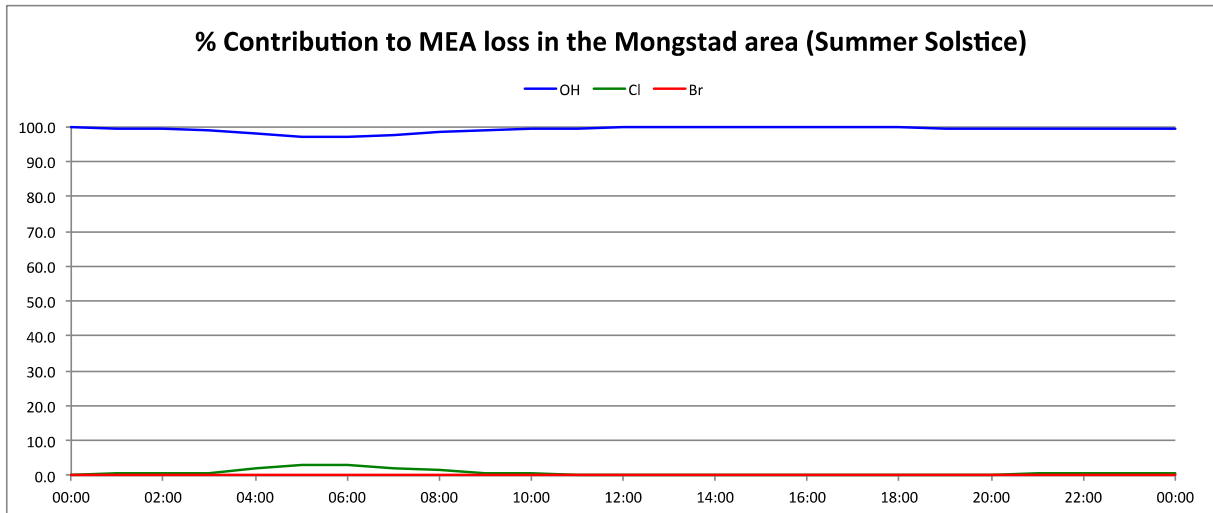


Figure 5.34. Box model results for 2-aminoethanol (MEA) gas phase loss due to reaction with OH radicals, and Cl and Br atoms in the Mongstad area around Summer Solstice.

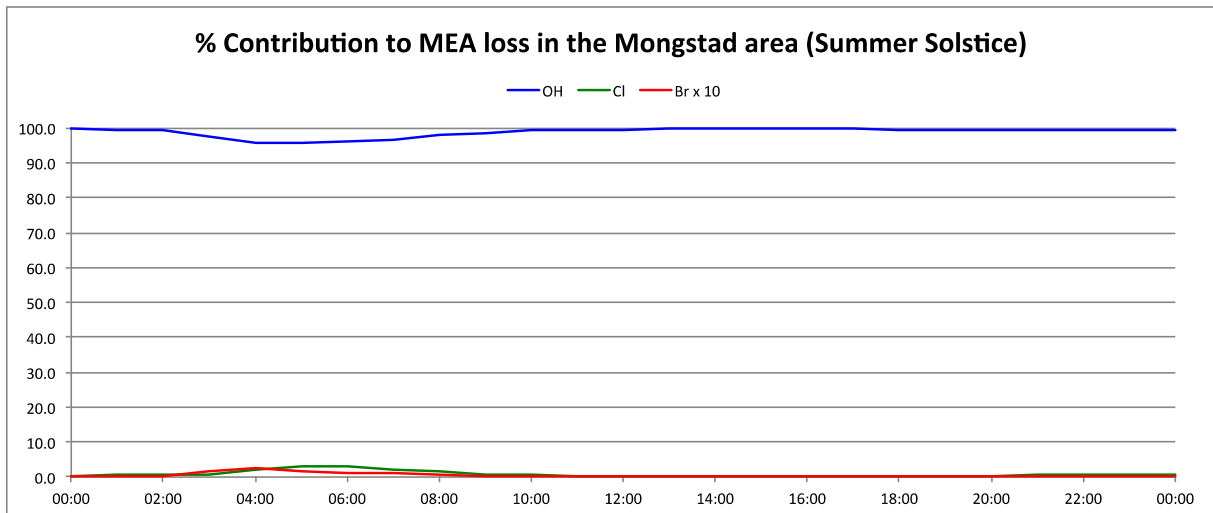


Figure 5.35. Box model results for 2-aminoethanol (MEA) gas phase loss due to reaction with OH radicals, and Cl and Br atoms in the Mongstad area around Summer Solstice. Br concentration enhanced by a factor of 10.

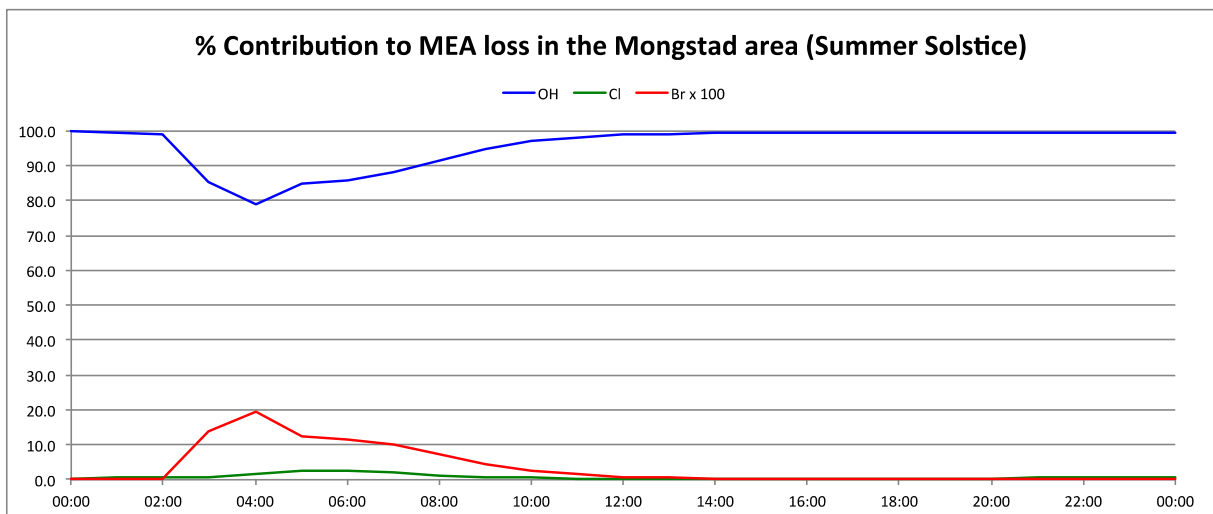


Figure 5.36. Box model results for 2-aminoethanol (MEA) gas phase loss due to reaction with OH radicals, and Cl and Br atoms in the Mongstad area around Summer Solstice. Br concentration enhanced by a factor of 100.

## 6 CONCLUSIONS AND RECOMMENDATIONS

The *Atmospheric Chemistry – Chlorine Chemistry* project concluded: Br atom reactions with amines could be more important than the corresponding Cl atom reactions in the Mongstad area. Model calculations indicate that Br atom concentrations in the Mongstad area could be at least an order of magnitude larger than the Cl atom concentrations. Since the Br and Cl atom reactions are expected to proceed in a similar fashion, *i.e.* via an  $R_3N^*X$  adduct, the rate coefficients may be of the same magnitude.

The present theoretical study has conclusively determined that the Cl and Br atom reactions with amines indeed both do proceed via adduct formation, but that the reactions otherwise differ such that it is not possible to extract any obvious correlation from the limited data available.

The Br atom reactions with amines are endothermic and endergonic, and only *upper* limits to the rate coefficients for Br atom reaction with amines can be obtained from the theoretical calculations.

*Even with very conservative upper limits to the Br atom rate coefficients for reaction with methyl-, dimethyl-, trimethylamine and MEA, and an order of 2 higher Br atom concentration in the Mongstad area than suggested in the Tel-Tek report no. 2211030-CC02, Halogen Chemistry in the Mongstad Region: Literature Study and Model Simulations,<sup>1</sup> the only amine that may react to any significant degree with Br atoms will be trimethylamine (and most like also other tertiary amines).*

As illustrated in sections 5.1 through 5.3 there are large diurnal variations in the atmospheric amine removal by Br atoms. Since the Br atom concentration essentially is correlated to the daytime OH radical concentration, an extra loss can be accounted for by a small increase of the OH rate coefficient in dispersion models.

Considering that upper estimates for the Br rate coefficients for reactions with amines, and that upper estimates for the Br atom concentration in the Mongstad region have been used in the modelling it is concluded that Br atom reactions will not constitute an important atmospheric loss process in the Mongstad area.

<i>Recommendation:</i>	<i>No need for further studies on amine + Br reactions. No need to include amine+Br reactions in dispersion modelling.</i>
------------------------	--

## 7 LITERATURE

1. Wolke, R.; Schrödner, R. *Specification of atmospheric conditions: Halogen Chemistry in the Mongstad Region: Literature Study and Model Simulations*; Report no. 2211030-CC02; Tel-Tek: 2011.
2. Frisch, M. J.; Trucks, G. W.; Schlegel, H. B.; Scuseria, G. E.; Robb, M. A.; Cheeseman, J. R.; Montgomery, J. A., Jr.; Vreven, T.; Kudin, K. N.; Burant, J. C.; Millam, J. M.; Iyengar, S. S.; Tomasi, J.; Barone, V.; Mennucci, B.; Cossi, M.; Scalmani, G.; Rega, N.; Petersson, G. A.; Nakatsuji, H.; Hada, M.; Ehara, M.; Toyota, K.; Fukuda, R.; Hasegawa, J.; Ishida, M.; Nakajima, T.; Honda, Y.; Kitao, O.; Nakai, H.; Klene, M.; Li, X.; Knox, J. E.; Hratchian, H. P.; Cross, J. B.; Adamo, C.; Jaramillo, J.; Gomperts, R.; Stratmann, R. E.; Yazyev, O.; Austin, A. J.; Cammi, R.; Pomelli, C.; Ochterski, J. W.; Ayala, P. Y.; Morokuma, K.; Voth, G. A.; Salvador, P.; Dannenberg, J. J.; Zakrzewski, V. G.; Dapprich, S.; Daniels, A. D.; Strain, M. C.; Farkas, O.; Malick, D. K.; Rabuck, A. D.; Raghavachari, K.; Foresman, J. B.; Ortiz, J. V.; Cui, Q.; Baboul, A. G.; Clifford, S.; Cioslowski, J.; Stefanov, B. B.; Liu, G.; Liashenko, A.; Piskorz, P.; Komaromi, I.; Martin, R. L.; Fox, D. J.; Keith, T.; Al-Laham, M. A.; Peng, C. Y.; Nanayakkara, A.; Challacombe, M.; Gill, P. M. W.; Johnson, B.; Chen, W.; Wong, M. W.; Gonzalez, C.; Pople, J. A. *Gaussian 03, Revision B.03*, Gaussian, Inc.: Pittsburgh PA, 2003.
3. Frisch, M. J.; Trucks, G. W.; Schlegel, H. B.; Scuseria, G. E.; Robb, M. A.; Cheeseman, J. R.; Scalmani, G.; Barone, V.; Mennucci, B.; Petersson, G. A.; Nakatsuji, H.; Caricato, M.; Li, X.; Hratchian, H. P.; Izmaylov, A. F.; Bloino, J.; Zheng, G.; Sonnenberg, J. L.; Hada, M.; Ehara, M.; Toyota, K.; Fukuda, R.; Hasegawa, J.; Ishida, M.; Nakajima, T.; Honda, Y.; Kitao, O.; Nakai, H.; Vreven, T.; Montgomery, J., J. A.; ; Peralta, J. E.; Ogliaro, F.; Bearpark, M.; Heyd, J. J.; Brothers, E.; Kudin, K. N.; Staroverov, V. N.; Kobayashi, R.; Normand, J.; Raghavachari, K.; Rendell, A.; Burant, J. C.; Iyengar, S. S.; Tomasi, J.; Cossi, M.; Rega, N.; Millam, J. M.; Klene, M.; Knox, J. E.; Cross, J. B.; Bakken, V.; Adamo, C.; Jaramillo, J.; Gomperts, R.; Stratmann, R. E.; Yazyev, O.; Austin, A. J.; Cammi, R.; Pomelli, C.; Ochterski, J. W.; Martin, R. L.; Morokuma, K.; Zakrzewski, V. G.; Voth, G. A.; Salvador, P.; Dannenberg, J. J.; Dapprich, S.; Daniels, A. D.; Farkas, O.; Foresman, J. B.; Ortiz, J. V.; Cioslowski, J.; Fox, D. J. *Gaussian 09, Revision B.01*, Gaussian, Inc., Wallingford CT: 2009.
4. Head-Gordon, M.; Pople, J. A.; Frisch, M. J., MP2 Energy evaluation by direct methods. *Chemical Physics Letters* **1988**, *153* (6), 503-506.
5. Frisch, M. J.; Head-Gordon, M.; Pople, J. A., A direct MP2 gradient-method. *Chemical Physics Letters* **1990**, *166* (3), 275-280.
6. Frisch, M. J.; Head-Gordon, M.; Pople, J. A., Semidirect algorithms for the MP2 energy and gradient. *Chemical Physics Letters* **1990**, *166* (3), 281-289.
7. Head-Gordon, M.; Head-Gordon, T., Analytical MP2 frequencies without 5th-order storage - Theory and application to bifurcated hydrogen-bonds in the water hexamer. *Chemical Physics Letters* **1994**, *220* (1-2), 122-128.
8. Saebo, S.; Almlof, J., Avoiding the integral storage bottleneck in LCAO calculations of electron correlation. *Chemical Physics Letters* **1989**, *154* (1), 83-89.
9. Pople, J. A.; Krishnan, R.; Schlegel, H. B.; Binkley, J. S., Electron correlation theories and their application to study of simple reaction potential surfaces. *International Journal of Quantum Chemistry* **1978**, *14* (5), 545-560.
10. Cizek, J., Use of the cluster expansion and the technique of diagrams in calculations of correlation effects in atoms and molecules. *Advan. Chem. Phys.* **1969**, *14*, 35-89.
11. Purvis, G. D.; Bartlett, R. J., A full coupled-cluster singles and doubles model - The inclusion of disconnected tripples. *Journal of Chemical Physics* **1982**, *76* (4), 1910-1918.

12. Scuseria, G. E.; Janssen, C. L.; Schaefer, H. F., III, An efficient reformulation of the closed-shell coupled cluster single and double excitation (CCSD) equations. *J. Chem. Phys.* **1988**, *89*, 7382-7.
13. Scuseria, G. E.; Schaefer, H. F., III, Is coupled cluster singles and doubles (CCSD) more computationally intensive than quadratic configuration interaction (QCISD)? *J. Chem. Phys.* **1989**, *90*, 3700-3.
14. Pople, J. A.; Head-Gordon, M.; Raghavachari, K., Quadratic configuration interaction. A general technique for determining electron correlation energies. *J. Chem. Phys.* **1987**, *87*, 5968-75.
15. Kendall, R. A.; Dunning, T. H., Jr.; Harrison, R. J., Electron affinities of the first-row atoms revisited. Systematic basis sets and wave functions. *J. Chem. Phys.* **1992**, *96* (9), 6796-806.
16. Dunning, T. H., Jr., Gaussian basis sets for use in correlated molecular calculations. I. The atoms boron through neon and hydrogen. *J. Chem. Phys.* **1989**, *90* (2), 1007-23.
17. Peterson, K. A.; Woon, D. E.; Dunning, T. H., Jr., Benchmark calculations with correlated molecular wave functions. IV. The classical barrier height of the H + H<sub>2</sub> -> H<sub>2</sub> + H reaction. *J. Chem. Phys.* **1994**, *100*, 7410-15.
18. Wilson, A. K.; van, M. T.; Dunning, T. H., Jr., Gaussian basis sets for use in correlated molecular calculations. VI. Sextuple zeta correlation consistent basis sets for boron through neon. *J. Mol. Struct.: THEOCHEM* **1996**, *388*, 339-349.
19. Gonzalez, C.; Schlegel, H. B., Reaction path following in mass-weighted internal coordinates. *J. Phys. Chem.* **1990**, *94* (14), 5523-7.
20. Ralchenko, Y.; Jou, F.-C.; Kelleher, D. E.; Kramida, A. E.; Musgrove, A. R., J.; Wiese, W. L.; Olsen, K., NIST Atomic Spectra Database, version 3.1.2. National Institute of Standards and Technology: Gaithersburg, MD.: 2007.
21. Schatz, G. C., Influence of Atomic Fine-Structure on Bimolecular Rate Constants - the Cl(<sup>2</sup>P) + HCl Reaction. *Journal of Physical Chemistry* **1995**, *99* (19), 7522-7529.
22. Montgomery, J. A.; Frisch, M. J.; Ochterski, J. W.; Petersson, G. A., A complete basis set model chemistry. VI. Use of density functional geometries and frequencies. *Journal of Chemical Physics* **1999**, *110* (6), 2822-2827.
23. Curtiss, L. A.; Raghavachari, K.; Redfern, P. C.; Rassolov, V.; Pople, J. A., Gaussian-3 (G3) theory for molecules containing first and second-row atoms. *Journal of Chemical Physics* **1998**, *109* (18), 7764-7776.
24. Curtiss, L. A.; Redfern, P. C.; Raghavachari, K., Gaussian-4 theory. *Journal of Chemical Physics* **2007**, *126*, 084108.
25. Becke, A. D., Density-functional thermochemistry. III. The role of exact exchange. *J. Chem. Phys.* **1993**, *98*, 5648-5652.
26. Lee, C.; Yang, W.; Parr, R. G., Development of the Colle-Salvetti correlation-energy formula into a functional of the electron density. *Phys. Rev. B: Condens. Matter* **1988**, *37*, 785-9.
27. Vosko, S. H.; Wilk, L.; Nusair, M., Accurate spin-dependent electron liquid correlation energies for local spin-density calculations - a critical analysis. *Canadian Journal of Physics* **1980**, *58* (8), 1200-1211.
28. Stephens, P. J.; Devlin, F. J.; Chabalowski, C. F.; Frisch, M. J., Ab Initio Calculation of Vibrational Absorption and Circular Dichroism Spectra Using Density Functional Force Fields. *J. Phys. Chem.* **1994**, *98*, 11623-7.
29. Curtiss, L. A.; Redfern, P. C.; Raghavachari, K., Assessment of Gaussian-3 and density-functional theories on the G3/05 test set of experimental energies. *J. Chem. Phys.* **2005**, *123*, 124107/1-124107/12.

30. Chase, M. W.; National Institute of, S.; Technology, *NIST-JANAF thermochemical tables*. American Chemical Society ; American Institute of Physics for the National Institute of Standards and Technology: [Washington, D.C.]; Woodbury, N.Y., 1998.
31. Takhistov, V. V., *Organic Mass Spectrometry (in Russian)*. Nauka: Leningrad, 1990.
32. McMillen, D. F.; Golden, D. M., Hydrocarbon Bond-Dissociation Energies. *Annual Review of Physical Chemistry* **1982**, *33*, 493-532.
33. Rudic, S.; Murray, C.; Harvey, J. N.; Orr-Ewing, A. J., The product branching and dynamics of the reaction of chlorine atoms with methylamine. *Physical Chemistry Chemical Physics* **2003**, *5* (6), 1205-1212.
34. Curtiss, L. A.; Raghavachari, K.; Trucks, G. W.; Pople, J. A., Gaussian-2 Theory for Molecular-Energies of 1st-Row and 2nd-Row Compounds. *Journal of Chemical Physics* **1991**, *94* (11), 7221-7230.
35. Rozenberg, M.; Loewenschuss, A.; Nielsen, C. J., H-Bonded Clusters in the Trimethylamine/Water System: A Matrix Isolation and Computational Study. *The Journal of Physical Chemistry A* **2012**, *116* (16), 4089-4096.
36. Atkinson, R.; Perry, R. A.; Pitts, J. N., Jr., Rate constants for the reaction of the hydroxyl radical with methanethiol and methylamine over the temperature range 299-426 K. *Journal of Chemical Physics* **1977**, *66* (4), 1578-81.
37. Carl, S. A.; Crowley, J. N., Sequential two (blue) photon absorption by NO<sub>2</sub> in the presence of H<sub>2</sub> as a source of OH in pulsed photolysis kinetic studies: Rate constants for reaction of OH with CH<sub>3</sub>NH<sub>2</sub>, (CH<sub>3</sub>)<sub>2</sub>NH, (CH<sub>3</sub>)<sub>3</sub>N, and C<sub>2</sub>H<sub>5</sub>NH<sub>2</sub> at 295 K. *J. Phys. Chem. A* **1998**, *102* (42), 8131-8141.
38. Laine, P.; Nicovich, J. M.; Wine, P. H. *Atmospheric Chemistry - Chlorine Chemistry. Kinetic Studies of the Reactions of Cl Atoms with Amines*; Report no. 2211030-CC04; Tel-Tek: 2011.
39. Atkinson, R.; Perry, R. A.; Pitts, J. N., Jr., Rate constants for the reactions of the hydroxyl radical with dimethylamine, trimethylamine, and ethylamine over the temperature range 298-426 K. *Journal of Chemical Physics* **1978**, *68* (4), 1850-3.
40. Nielsen, C. J.; D'Anna, B.; Bossi, R.; Bunkan, A. J. C.; Dithmer, L.; Glasius, M.; Hallquist, M.; Hansen, A. M. K.; Lutz, A.; Salo, K.; Maguta, M. M.; Nguyen, Q.; Mikoviny, T.; Müller, M.; Skov, H.; Sarrasin, E.; Stenstrøm, Y.; Tang, Y.; Westerlund, J.; Wisthaler, A. *Atmospheric Degradation of Amines (ADA)*; ISBN 978-82-992954-7-5, <http://urn.nb.no/URN:NBN:no-30510>; University of Oslo: Oslo, 2012.
41. Onel, L.; Blitz, M. A.; Seakins, P. W., Direct Determination of the Rate Coefficient for the Reaction of OH Radicals with Monoethanol Amine (MEA) from 296 to 510 K. *The Journal of Physical Chemistry Letters* **2012**, *3* (7), 853-856.
42. Wolke, R.; Schrödner, R. *Atmospheric Chemistry – Dark Chemistry. Nighttime Chemistry in the Mongstad Area: Literature Study and Model Simulations*; Report no. 2211030-DC01; Tel-Tek: 2011.
43. Nielsen, C. J.; D'Anna, B.; Karl, M.; Aursnes, M.; Boreave, A.; Bossi, R.; Bunkan, A. J. C.; Glasius, M.; Hansen, A.-M. K.; Hallquist, M.; Kristensen, K.; Mikoviny, T.; Maguta, M. M.; Müller, M.; Nguyen, Q.; Westerlund, J.; Salo, K.; Skov, H.; Stenstrøm, Y.; Wisthaler, A. *Summary Report: Photo-oxidation of Methylamine, Dimethylamine and Trimethylamine. Climit project no. 201604*; NILU OR 2/2011, ISBN 978-82-425-2357-0; NILU: 2011.
44. Aston, J. G.; Siller, C. W.; Messerly, G. H., Heat capacities and entropies of organic compounds. III. Methylamine from 11.5 °K. to the boiling point. Heat of vaporization and vapor pressure. The entropy from molecular data. *J. Am. Chem. Soc.* **1937**, *59*, 1743-51.

45. Aston, J. G.; Eidinoff, M. L.; Forster, W. S., The heat capacity and entropy, heats of fusion and vaporization and the vapor pressure of dimethylamine. *J. Am. Chem. Soc.* **1939**, *61*, 1539-43.
46. Griller, D.; Lossing, F. P., Thermochemistry of  $\alpha$ -aminoalkyl radicals. *J. Am. Chem. Soc.* **1981**, *103* (6), 1586-1587.
47. Aston, J. G.; Sagenkahn, M. L.; Szasz, G. J.; Moessen, G. W.; Zuhr, H. F., The heat capacity and entropy, heats of fusion and vaporization and the vapor pressure of Me<sub>3</sub>N. The entropy from spectroscopic and molecular data. *J. Am. Chem. Soc.* **1944**, *66*, 1171-7.

**ANNEX 1. EXPERIMENTAL ENTHALPIES OF FORMATION**

The experimental enthalpies of formation for methyl-, dimethyl-, trimethylamine, and the various radicals of these at 298.15 K are summarised in

Table A.1. The enthalpies of formation of Cl, Br, HCl and HBr are summarised in Table A.2.

Table A.1. Enthalpies of formation of amines, alkyl amine radicals, and amino radicals.

Species	$\Delta_f H_{298}^\theta / \text{kJ} \cdot \text{mol}^{-1}$	Reference
CH <sub>3</sub> NH <sub>2</sub>	-23.0	44
CH <sub>2</sub> NH <sub>2</sub>	149.4	32 (Review)
CH <sub>3</sub> NH	177.4	32 (Review)
(CH <sub>3</sub> ) <sub>2</sub> NH	-18.6	45
CH <sub>3</sub> NHCH <sub>2</sub>	125.5	46
(CH <sub>3</sub> ) <sub>2</sub> N	145.2	32 (Review)
(CH <sub>3</sub> ) <sub>3</sub> NH	-23.7	47
(CH <sub>3</sub> ) <sub>2</sub> NCH <sub>2</sub>	109.6	46

Table A.2. Enthalpies of formation of amines, alkyl amine radicals, and amino radicals.

Species	$\Delta_f H_{298}^\theta / \text{kJ} \cdot \text{mol}^{-1}$	Ground state term and Spin-Orbit splitting /cm <sup>-1</sup>	Reference
H	218.00 ± 0.01	<sup>2</sup> S <sub>1/2</sub>	30 (Review)
Cl	121.302 ± 0.008	<sup>2</sup> P <sub>3/2</sub> 0 g=4; <sup>2</sup> P <sub>1/2</sub> 882.36 g=2	30 (Review)
HCl	-92.31 ± 0.21		30 (Review)
Br	117.920 ± 0.006	<sup>2</sup> P <sub>3/2</sub> 0 g=4; <sup>2</sup> P <sub>1/2</sub> 3685.24 g=2	30 (Review)
HBr	-36.44 ± 0.17		30 (Review)